Supporting Information

New D–π–A Dyes Based on Indolo[3,2,1-*jk*]carbazole and Thienopyrrolo[3,2,1-*jk*]carbazole for Application in Dye-Sensitized Solar Cells

Grażyna Szafraniec-Gorol[1*], Paweł Gnida[2], Sonia Kotowicz[1], Paweł Czulkin[3], Ewa Schab-Balcerzak[1,2]

[1] *Institute of Chemistry, University of Silesia, 9 Szkolna Str., 40-006 Katowice, Poland*

[2] *Centre of Polymer and Carbon Materials, Polish Academy of Sciences, 34 M. Curie-Sklodowska Str., 41-819 Zabrze, Poland*

[3] *Faculty of Chemistry, Silesian University of Technology, 9 Strzody, Gliwice 44-100, Poland*

Materials and measurements

The NMR spectra were recorded on a Bruker Avance 500 MHz instrument by using $CDCl_3$ and DMSO-d6 as solvents. Thermogravimetric analysis (TGA) was performed on a Mettler Toledo TGA STARe system at a heating rate of 10 °C·min-1 under a constant stream of nitrogen (20 ml·min^{-1}). UV-Vis spectra were measured by using Shimadzu UV-1900 UV-Vis spectrophotometer at room temperature with a conventional 1.0 cm quartz cell. The steady-state emission and excitation spectra were measured by using the spectrofluorometer FS5, Edinburgh Instruments. The quantum yields of fluorescence (Φ) were determined by absolute method in room temperature, using the integrating sphere with solvent as a blank.on the using spectrofluoremeter FS5 Edinburgh Instruments using 450W Xe arc lamp as a light source and PMT in cooled housing as a detector. Compounds were excited in the wavelength corresponding to the absorption wavelength of the compounds. The time-resolved measurement has been prepared at optically diluted solutions at room temperature using the time correlated single photon counting methods on the spectrofluoremeter FS5 Edinburgh Instruments. Excitation wavelengths were obtained using the picosecond pulsed diode EPLED-475 nm with 100 ns pulse period as light sources.

Additionally, for the analysis of fluorescence decay, an instrument response function needs to be obtained. The IRF was designated using LUDOX solution as a standard at 475 nm.
The electrochemical measurements were carried out using differential pulse voltammetry (DPV) and the cyclic voltammetry (CV) on an Eco ChemieAutolab PGSTAT128n potentiostat. All experiments were performed in dichloromethane (CH_2Cl_2, DCM, Sigma-Aldrich, HPLC) with a sample concentration of $1 \cdot 10^{-3}$ mol·dm^{-3} and $1 \cdot 10^{-1}$ mol·dm^{-3} tetrabutylammonium hexafluorophosphate (Bu_4NPF_6, Sigma-Aldrich, 99%) as the supporting electrolyte. A conventional three-electrode system was used, consisting of a platinum working electrode (diameter 2.0 mm), a platinum coil counter electrode, and a silver wire quasi-reference electrode. To eliminate the water and oxygen influence the solutions were purged with argon for about 2 minutes before every measurement. All measurements were conducted at 23 ± 1˚C. Ferrocene/ferrocenium (Fc/Fc^+) was used as an internal standard (IP = -5.1 eV). [1]
The B3LYP and CAM-B3LYP exchange-correlation functionals implemented in the Gaussian 16 program were used for the DFT and TD-DFT calculations [2]. The polarisable continuum model (PCM) was implemented in all performed calculations [3]. Calculated isovalues for all orbitals were 0.02 e/bohr^3. The electronic spectra were presented visually by the Chemissian program [4].

Fluorine-doped tin oxide coated glass slides (FTOs, 7 Ω/sq, Sigma-Aldrich, Merck, Steinheim, Germany), 18NR-T titania paste (Greatcell Solar Materials, Queanbeyan East, NSW, Australia), platinum paste Platisol T/SP (Solaronix) surfactant (Hellmanex III, Hellma Analytics, Müllheim, Germany), 2-propanol (IPA), (POCH, Avantor, Gliwice, Poland), and titanium(IV) tetrachloride (Sigma-Aldrich, Merck) were used. Di-tetrabutylammonium *cis*-bis(isothiocyanato)bis(2,2′-bipyridyl-4,4′-dicarboxylato)ruthenium(II) (N719), and EL-HSE electrolyte were purchased from Sigma-Aldrich (Merck). *N,N-Dimethylformamide* (DMF) (Chempur, Piekary Śląskie, Poland), and chenodeoxycholic acid (CDCA) (Sigma-Aldrich, Merck) were applied in device preparation.
The current–voltage characteristics were measured using a Keithley 2400 SourceMeter (Tektronix, Inc., Beaverton, OR) in combination with dedicated software, and a PV Solutions solar simulator providing a standard light intensity of 100 mW cm^{-2} under AM 1.5G conditions (or for selected devices tested under illumination intensities in the range of 10 – 100 mW cm^{-2}). UV–Vis spectra for dye solutions and photoanodes were acquired using a Jasco V-750 UV–Vis–NIR spectrophotometer.

- Preparation of standard anodes with a mesoporous TiO_2 layer

Glass substrates coated with approximately 500 nm thick fluorine-doped tin oxide (FTO) layer were subjected to a multistep cleaning procedure. The substrates were first immersed in a 10% (v/v) aqueous solution of Hellmanex surfactant and sonicated for 15 min at 40 °C. Subsequently, they were thoroughly rinsed with distilled water and sonicated again under identical conditions. This rinsing and sonication cycle was repeated twice to ensure complete removal of contaminants. The substrates were then transferred to isopropanol (IPA) and sonicated for 5 min at 40 °C. Finally, the cleaned substrates were removed from IPA and allowed to dry under ambient conditions.
After complete drying, a TiO_2 paste (18NR-T, Greatcell Solar Materials) was deposited onto the FTO substrates via screen-printing. The number of successive layers was adjusted to obtain the desired TiO_2 film thickness. Each printed layer was subjected to a preheating step at 125 °C for 5 min to remove residual solvents and promote partial consolidation. After deposition of the final layer, the electrodes were sintered in a muffle furnace at 500 °C for 30 min. The resulting TiO_2-coated FTO substrates were subsequently allowed to cool naturally to room temperature.

- TiO_2 Blocking layer prepared from $TiCl_4$ (BL)

A 2 mol dm^{-3} stock solution was prepared from commercially available titanium(IV) tetrachloride ($TiCl_4$). The cleaned FTO substrates were placed in a Petri dish containing 29.25 mL of deionized water, followed by the addition of 0.75 mL of the 2 mol dm^{-3} $TiCl_4$ solution to obtain a final concentration of 0.05 mol dm^{-3}. The resulting solution was maintained at 70 °C for 30 min. After the $TiCl_4$ treatment, the substrates were removed from the solution, thoroughly rinsed with distilled water, and subsequently annealed in a furnace at 500 °C for 30 min.

- Platinum counter electrode

The counter electrode was fabricated on FTO glass substrates that were cleaned using the same protocol as for TiO_2 deposition. A commercial paste (Platisol T/SP) containing platinum nanoparticles was applied by screen printing to form a single uniform layer. The printed films were subsequently sintered in a muffle furnace at 450 °C for 30 min under ambient atmosphere.

- Fabrication of the DSSCs

The photoanodes were prepared by immersing the pre-fabricated anodes in a dye solution (or dye mixture) with a concentration of $3 \cdot 10^{-4}$ M. When a co-adsorbent was employed, an appropriate amount of CDCA was added to the dye solution to achieve a final concentration of 10 mM. Prior to immersion in the dye solution, the electrodes were heated at 80 °C for approximately 20 min. In each case, the electrodes were immersed in the respective solutions for 24 h. After this period, the photoanodes were removed, rinsed with MeOH to eliminate excess non-adsorbed dye molecules, and dried in air.
The DSSC was fabricated by assembling the pre-prepared photoanode and the counter electrode, with the inter-electrode gap filled with a commercial liquid electrolyte (EL-HSE) containing the I^-/I_3^- redox pair.

Synthesis

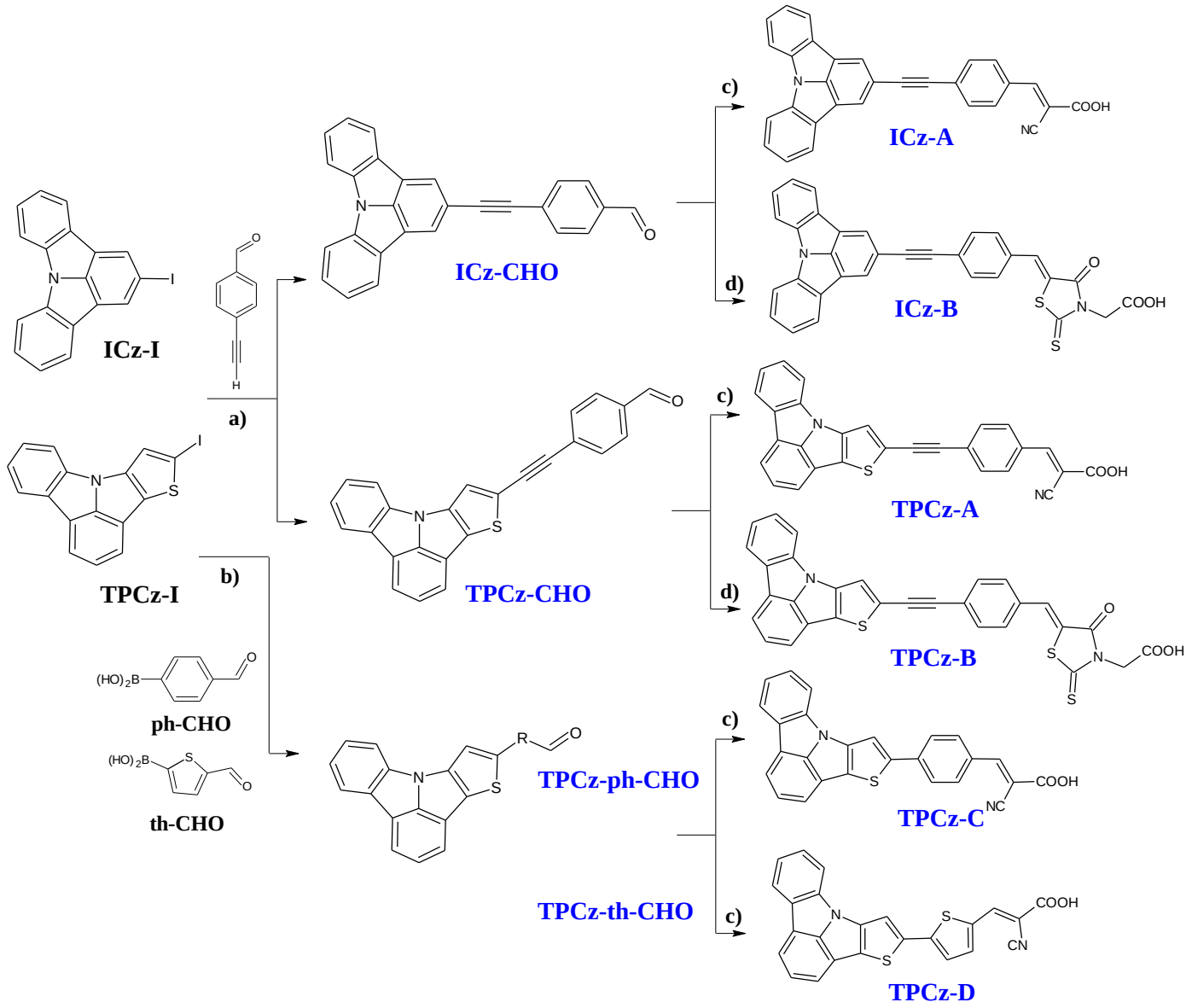

Scheme S1. Synthesis of **ICz-A** – **ICz-B** and **TPCz-A** – **TPCz-D** dyes**;** a) $[Pd(PPh_3)_4]$, CuI, NEt_3/THF, Ar, 70 °C, 24 h; b) $[Pd(PPh_3)_4]$, Na_2CO_3, $PhCH_3$/EtOH, Ar, 90 °C, 24 h; c) cyanoacetic acid, piperidine, $CHCl_3$/MeCN, Ar, 90 °C, 24 h; d) rhodanine-3-acetic acid, piperidine, EtOH, Ar, 80 °C, 24 h.

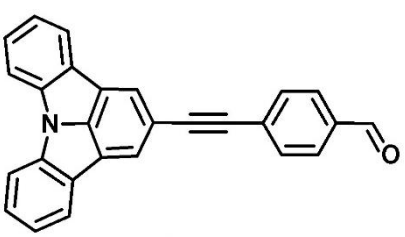

ICz-A: To a Schlenk flask equipped with a magnetic stir bar, 200 mg (0.54 mmol) 4-(indolo[3,2,1-*jk*]carbazol-2-yl)ethynyl)-benzaldehyde and 367 mg (4.32 mmol) cyanoacetic acid were loaded. The flask was evacuated and flushed with argon for three cycles. Next, a 20 mL mixture of MeCN/$CHCl_3$ (1:1) was added, and the mixture was evacuated and flushed with argon again. Then, 0.59 mL (5.94 mmol) piperidine was added, and the last time, the flask was flushed with argon and evacuated. The mixture was heated at 90 °C for 24 h. After being

cooled to room temperature, the mixture was evaporated under reduced pressure. Water and CH_2Cl_2 were added, and the crude product was extracted with CH_2Cl_2 with the addition of 4.5% HCl. The organic layer was collected and dried over anhydrous $MgSO_4$. After filtration, the solvent was removed under reduced pressure. The residue was purified by crystallization from a mixture of $CHCl_3$/MeOH, giving the orange solid state (174 mg, 0.40 mmol, yield = 74%). ^{1}H NMR (400 MHz, DMSO) δ 8.51 (s, 2H), 8.34 (t, *J* = 7.4 Hz, 4H), 8.24 (s, 1H), 8.08 (d, *J* = 8.2 Hz, 2H), 7.79 (d, *J* = 8.2 Hz, 2H), 7.68 (t, *J* = 7.7 Hz, 2H), 7.47 (t, *J* = 7.6 Hz, 2H). ^{13}C NMR (101 MHz, DMSO) δ 163.32, 143.15, 139.01, 132.29, 132.21, 130.99, 129.07, 128.41, 126.97, 124.52, 124.34, 123.09, 118.59, 117.65, 116.76, 113.52, 95.32, 87.72. ^{13}C NMR (101 MHz, DMSO) δ 163.26, 151.20, 143.19, 138.95, 132.29, 132.21, 130.99, 129.07, 128.41, 126.99, 124.58, 124.52, 124.34, 123.09, 118.59, 117.71, 116.76, 113.52, 95.36, 87.72. APCI(-)-HRMS: *m/z* calcd. for $C_{30}H_{15}N_2O_2$: 435.1139, $[M-H]^-$; found: 435.1145.

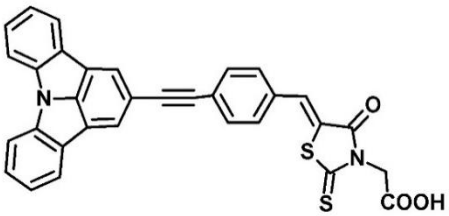

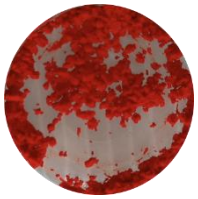

ICz-B: To a Schlenk flask equipped with a magnetic stir bar, 97 mg (0.26 mmol) 4-(indolo[3,2,1-*jk*]carbazol-2-yl)ethynyl)-benzaldehyde and 79 mg (0.42 mmol) rhodanine-3-acetic acid were loaded. The flask was evacuated and flushed with argon for three cycles. Next, 10 mL of ethanol was added, and the mixture was evacuated and flushed with argon again. Then, 0.1 mL (1.04 mmol) piperidine was added, and the last time, the flask was flushed with argon and evacuated. The mixture was heated at 80 °C for 24 h. After being cooled to room temperature, the mixture was evaporated under reduced pressure. Water and $CHCl_3$ were added, and the crude product was extracted with $CHCl_3$ with the addition of 4.5% HCl. The organic layer was collected and dried over anhydrous $MgSO_4$. After filtration, the solvent was removed under reduced pressure. The residue was purified by crystallization from a mixture of $CHCl_3$/MeOH, giving the red solid state (91 mg, 0.17 mmol, yield = 65%). ^{1}H NMR (400 MHz, DMSO) δ 8.51 (s, 2H), 8.35 (t, *J* = 6.8 Hz, 4H), 7.95 (s, 1H), 7.82 – 7.75 (m, 4H), 7.69 (t, *J* = 7.8 Hz, 2H), 7.47 (t, *J* = 7.6 Hz, 2H), 4.76 (s, 2H). ^{13}C NMR (101 MHz, DMSO) δ 167.71, 166.87, 156.20, 140.47, 139.05, 133.45, 132.94, 132.56, 131.64, 129.13, 128.42, 124.52, 124.48, 124.33, 123.09, 123.06, 122.89, 118.63, 116.77, 113.50, 95.58, 87.90, 45.55. APCI(-)-HRMS: *m/z* calcd. for $C_{32}H_{17}N_2O_3S_2$: 541.0686, $[M-H]^-$; found: 541.0677

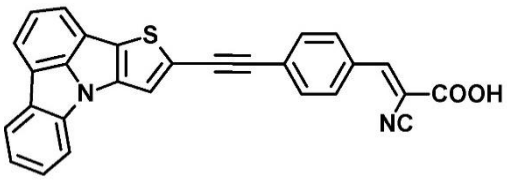

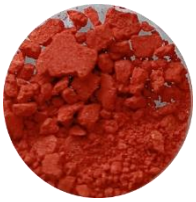

TPCz-A: To a Schlenk flask equipped with a magnetic stir bar, 100 mg (0.26 mmol) *p*-[(thieno[2′,3′:4,5]pyrrolo[3,2,1-jk]carbazol-5-yl)ethynyl]benzaldehyde and 177 mg (2.08 mmol) cyanoacetic acid were loaded. The flask was evacuated and flushed with argon for three cycles. Next, a 30 mL mixture of $CHCl_3$/MeCN (2:1) was added, and the mixture was evacuated and flushed with argon again. Then, 0.28 mL (2.86 mmol) piperidine was added, and the last time, the flask was flushed with argon and evacuated. The mixture was heated at 80 °C for 24 h. After being cooled to room temperature, the mixture was evaporated under reduced pressure. Water and $CHCl_3$ were added, and the crude product was extracted with $CHCl_3$ with the addition of 4.5% HCl. The organic layer was collected and dried over anhydrous $MgSO_4$. After filtration, the solvent was removed under reduced pressure. The residue was purified by crystallization from a mixture of $CHCl_3$/MeOH, giving the red solid state (50 mg, 0.11 mmol, yield = 42%). ^{1}H NMR (400 MHz, DMSO) δ 8.48 (s, 1H), 8.37 (s, 1H), 8.27 (d, *J* = 7.7 Hz, 1H), 8.23

(d, *J* = 8.1 Hz, 1H), 8.14 (m, 2H), 8.07 (d, *J* = 7.6 Hz, 1H), 7.96 (s, 1H), 7.81 (d, *J* = 8.1 Hz, 2H), 7.63 (m, 2H), 7.42 (m, 1H). ^{13}C NMR (126 MHz, DMSO) δ 149.98, 145.25, 139.90, 138.27, 132.20, 132.11, 131.33, 128.99, 128.63, 127.93, 127.90, 126.19, 125.19, 124.27, 123.86, 123.65, 122.94, 120.01, 119.77, 119.76, 118.89, 116.85, 112.92, 98.49, 94.50, 87.91. APCI(-)-HRMS for $C_{28}H_{13}N_2O_2S$ calcd. for: 441.0698, $[M-H]^-$ found: 441.0710.

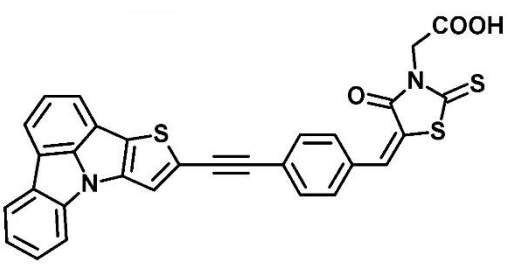

TPCz-B: To a Schlenk flask equipped with a magnetic stir bar, 150 mg (0.40 mmol) *p*-[(thieno[2′,3′:4,5]pyrrolo[3,2,1-jk]carbazol-5-yl)ethynyl]benzaldehyde and 122 mg (0.64 mmol) rhodanine-3-acetic acid were loaded. The flask was evacuated and flushed with argon for three cycles. Next, 20 mL of ethanol was added, and the mixture was evacuated and flushed with argon again. Then, 0.16 mL (1.6 mmol) piperidine was added, and the last time, the flask was flushed with argon and evacuated. The mixture was heated at 80 °C for 24 h. After being cooled to room temperature, the mixture was evaporated under reduced pressure. Water and $CHCl_3$ were added, and the crude product was extracted with $CHCl_3$ with the addition of 4.5% HCl. The organic layer was collected and dried over anhydrous $MgSO_4$. After filtration, the solvent was removed under reduced pressure. The residue was purified by crystallization from a mixture of $CHCl_3$/MeOH, yielding a deep-dark red solid (50 mg, 0.09 mmol, yield = 23%). ^{1}H NMR (400 MHz, DMSO) δ 8.47 (s, 1H), 8.27 (d, *J* = 7.4 Hz, 1H), 8.23 (d, *J* = 7.9 Hz, 1H), 8.15 (d, *J* = 7.2 Hz, 1H), 8.07 (d, *J* = 7.6 Hz, 1H), 7.93 (s, 1H), 7.78 (m, 4H), 7.63 (m, 2H), 7.42 (m, 1H), 4.71 (s, 2H). ^{13}C NMR (126 MHz, DMSO) δ 166.84, 145.27, 145.10, 139.93, 138.36, 133.22, 132.49, 131.78, 131.63, 130.42, 129.01, 127.92, 127.77, 125.10, 124.54, 124.42, 124.29, 123.80, 123.29, 122.98, 119.81, 119.77, 118.79, 118.23, 116.93, 116.89, 112.92, 94.61, 87.62, 45.78. APCI(-)-HRMS: *m/z* calcd. for $C_{30}H_{15}N_2O_3S_3$: 547.0250, $[M-H]^-$; found: 547.0234

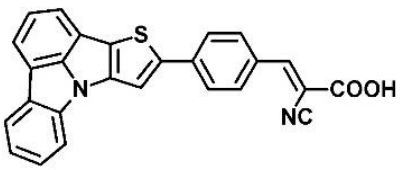

TPCz-C: To a Schlenk flask equipped with a magnetic stir bar, 150 mg (0.42 mmol) p-(thieno[2′,3′:4,5]pyrrolo[3,2,1-jk]carbazol-5-yl)benzaldehyde and 290 mg (3.36 mmol) cyanoacetic acid were loaded. The flask was evacuated and flushed with argon for three cycles. Next, a 30 mL mixture of $CHCl_3$/MeCN (1:1) was added, and the mixture was evacuated and flushed with argon again. Then, 0.45 mL (4.62 mmol) piperidine was added, and the last time, the flask was flushed with argon and evacuated. The mixture was heated at 90 °C for 24 h. After being cooled to room temperature, the mixture was evaporated under reduced pressure. Water and $CHCl_3$ were added, and the crude product was extracted with $CHCl_3$ with the addition of 4.5% HCl. The organic layer was collected and dried over anhydrous MgSO4. After filtration, the solvent was removed under reduced pressure. The residue was purified by crystallization from a mixture of $CHCl_3$/MeOH, yielding a deep-dark red solid (148 mg, 0.35 mmol, yield = 83%). ^{1}H NMR (500 MHz, DMSO) δ 8.71 (s, 1H), 8.33 (s, 1H), 8.26 (d, J = 7.5 Hz, 1H), 8.23 – 8.18 (m, 1H), 8.16 (s, 1H), 8.14 (s, 1H), 8.11 (d, *J* = 7.2 Hz, 1H), 8.04 (d, *J* = 6.6 Hz, 3H), 7.65 (t, *J* = 7.6 Hz,

1H), 7.61 (t, *J* = 7.4 Hz, 1H), 7.42 (t, *J* = 7.3 Hz, 1H). ^{13}C NMR (126 MHz, DMSO) δ 163.87, 153.74, 145.03, 144.58, 141.68, 139.13, 138.26, 132.22, 131.18, 130.78, 129.13, 128.86, 127.80, 127.51, 125.79, 124.20, 123.93, 123.89, 122.81, 119.66, 119.36, 117.19, 116.82, 112.68, 111.80, 103.33. ESI(-)-HRMS : *m/z* calcd. for $C_{26}H_{13}N_2O_2S$: 417.0698, $[M-H]^-$; found: 417.0693.

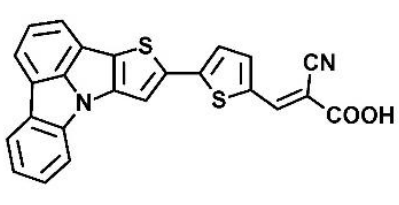

TPCz-D: To a Schlenk flask equipped with a magnetic stir bar, 144 mg (0.40 mmol) 5-(thieno[2′,3′:4,5]pyrrolo[3,2,1-jk]carbazol-5-yl)thiophene-2-carboxaldehyde and 273 mg (3.2 mmol) cyanoacetic acid were loaded. The flask was evacuated and flushed with argon for three cycles. Next, a 30 mL mixture of $CHCl_3$/MeCN (1:1) was added, and the mixture was again evacuated and flushed with argon. Then, 0.44 mL (4.4 mmol) piperidine was added, and the last time, the flask was flushed with argon and evacuated. The mixture was heated at 90 °C for 24 h. After being cooled to room temperature, the mixture was evaporated under reduced pressure. Water and $CHCl_3$ were added, and the crude product was extracted with $CHCl_3$ with the addition of 4.5% HCl. The organic layer was collected and dried over anhydrous MgSO4. After filtration, the solvent was removed under reduced pressure. The residue was purified by crystallization from a mixture of $CHCl_3$/MeOH, giving the deep-dark red solid state (147 mg, 0.35 mmol, yield = 86%). ^{1}H NMR (500 MHz, DMSO) δ 8.48 (d, *J* = 11.5 Hz, 1H), 8.33 – 8.31 (m, 1H), 8.25 (d, *J* = 7.6 Hz, 1H), 8.21 (s, 1H), 8.11 (d, *J* = 7.3 Hz, 1H), 8.01 (d, *J* = 7.5 Hz, 1H), 7.79 (d, *J* = 3.8 Hz, 1H), 7.62 – 7.59 (m, 3H), 7.42 (ddd, *J* = 7.8, 4.9, 1.0 Hz, 1H). ^{13}C NMR (126 MHz, DMSO) δ 164.63, 144.51, 143.34, 141.75, 141.15, 138.54, 138.23, 137.80, 136.08, 134.03, 130.79, 129.00, 127.83, 125.10, 124.27, 123.74, 123.20, 122.90, 119.59, 119.52, 119.29, 116.94, 112.90, 111.23. ESI(-)-HRMS : *m/z* calcd. for $C_{24}H_{11}N_2O_2S_2$: 423.0262, $[M-H]^-$; found: 423.0258.

ICz-I - 4-(indolo[3,2,1-*jk*]carbazol-2-yl)ethynyl)-benzaldehyde: A solution of indolo[3,2,1-jk]carbazole (4.0 g, 16.59 mmol) in 180 ml of mixture of $CH_3COOH/CHCl_3$ (2:1, v:v) was stirred under argon for 30 min. After this time, 1.0 eq. (3.71 g) NIS was added in small portions (in around 1 hour) to a constantly stirred solution. Next, the mixture was stirred at room temperature for 20 h. After this time, the solid was filtered and washed with H_2O, EtOH, and Et_2O. The 2-iodoindolo[3,2,1-jk]carbazole was obtained as a white solid (4.07 g, 11.09 mmol, yield = 66%). ^{1}H NMR (400 MHz, $CDCl_3$) δ 8.37 (s, 2H), 8.09 (d, *J* = 7.7 Hz, 2H), 7.90 (d, *J* = 8.1 Hz, 2H), 7.65 – 7.56 (m, 2H), 7.39 (t, *J* = 7.4 Hz, 2H). ^{13}C NMR (101 MHz, $CDCl_3$) δ 141.88, 138.90, 129.15, 127.38, 123.32, 122.27, 122.01, 119.55, 115.72, 112.26.

TPCz-I - 5-iodo-thieno[2′,3′:4,5]pyrrolo[3,2,1-jk]carbazole: A solution of thieno[2′,3′:4,5]-pyrrolo[3,2,1-jk]carbazole (0.88 g, 3.58 mmol) in 70 ml of mixture of $CH_3COOH/CHCl_3$ (2:5, v:v) was stirred under argon for 30 min. After this time, 1.0 eq. (0.88 g) NIS was added in small portions (in around 0.5 hour) to a constantly stirred solution. Next, the mixture was stirred at room temperature for 20 h. After this time, the solid was filtered and washed with H_2O, EtOH, and Et_2O. 5-Iodo-thieno[2′,3′:4,5]pyrrolo[3,2,1-jk]carbazole was obtained as a beige solid state (0.92 g, 2.47 mmol, yield = 69%). ^{1}H NMR (400 MHz, $CDCl_3$) δ 8.10 (d, *J* = 7.6 Hz, 1H), 7.96 (d, *J* = 7.6 Hz, 1H), 7.80 (d, *J* = 7.6 Hz, 1H), 7.69 (m, 2H), 7.55 (d, *J* = 7.6 Hz, 1H), 7.51 (d, *J* = 8.0 Hz, 1H), 7.35 (m,

1H). ^{13}C NMR (126 MHz, $CDCl_3$) δ 144.14, 139.97, 138.29, 129.37, 128.14, 126.81, 123.22, 123.10, 121.93, 120.92, 119.83, 118.23, 118.00, 116.87, 111.35, 75.04. HRMS(APCI) $[M+H]^+$ *m/z* calcd. for $C_{16}H_9INS$: 373.9500, $[M+H]^+$; found: 373.9474.

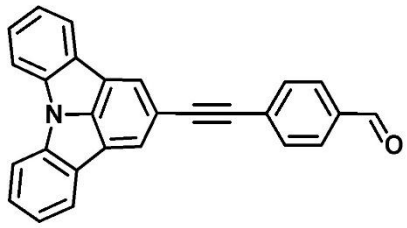

ICz-CHO - 4-(indolo[3,2,1-*jk*]carbazol-2-yl)ethynyl)-benzaldehyde: A solution of (270 mg; 0.74 mmol) 2-iodoindolo[3,2,1-*jk*]carbazole in 10 ml of a mixture of NEt_3/THF (7:3) was stirred under argon for 30 min. After this time, 85 mg of $[Pd(PPh_3)_4]$ (10%) and 14 mg of CuI (10%) were added, and the mixture was bubbled with argon for an additional 15 minutes. Next, a mixture of 1.2 eq. mol. 4-ethynylbenzaldehyde (115 mg; 0.88 mmol) in 6 mL of a mixture of NEt_3/THF (2:1) was injected through the septum, and the mixture was heated at 70 °C for 24h. After being cooled to room temperature, the mixture was evaporated under reduced pressure. The crude product was purified by silica gel column chromatography using hexane/dichloromethane (2:1) as eluent. The residue product was crystallized by hexane, giving the white solid state (110 mg; 0.297 mmol, yield = 40%). ^{1}H NMR (400 MHz, $CDCl_3$) δ 10.07 (s, 1H), 8.32 (s, 2H), 8.18 (d, *J* = 7.8 Hz, 2H), 7.95 (m, 4H), 7.78 (d, *J* = 7.8 Hz, 2H), 7.63 (t, *J* = 7.8 Hz, 2H), 7.43 (t, *J* = 7.4 Hz, 2H). ^{13}C NMR (101 MHz, $CDCl_3$) δ 191.45, 139.20, 135.14, 131.98, 131.92, 129.67, 129.47, 127.42, 123.71, 123.42, 122.34, 122.26, 118.51, 116.81, 112.39, 95.99, 86.94. HRMS (APCI): *m/z* calcd. for $C_{27}H_{16}NO$: 370.1226, $[M+H]^+$; found: 370.1235.

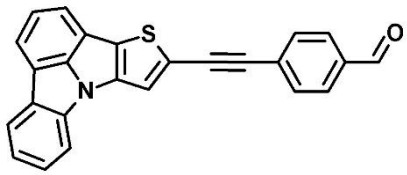

TPCz-CHO - *p*-[(thieno[2′,3′:4,5]pyrrolo[3,2,1-jk]carbazol-5-yl)ethynyl]benzaldehyde): A solution of (390 mg; 1.06 mmol) 5-iodo-thieno[2′,3′:4,5]pyrrolo[3,2,1-jk]carbazole in 24 ml of a mixture of NEt_3/THF (1:1) was stirred under argon for 30 min. After this time, 120 mg of $[Pd(PPh_3)_4]$ (10%) and 20 mg of CuI (10%) were added, and the mixture was bubbled with argon for an additional 15 minutes. Next, a mixture of 1.3 eq. mol. 4-ethynylbenzaldehyde (115 mg; 0.88 mmol) in 6 mL of THF was injected through the septum, and the mixture was heated at 70 °C for 24 h. After being cooled to room temperature, the mixture was evaporated under reduced pressure. The crude product was purified by silica gel column chromatography using hexane/dichloromethane (1:1) as eluent. The residue product was crystallized by hexane, giving the white solid state (360 mg; 0.96 mmol, yield = 90%). ^{11}H NMR (500 MHz, $CDCl_3$) δ 10.05 (s, 1H), 8.13 (dd, *J* = 7.2, 0.5 Hz, 1H), 7.99 (d, *J* = 7.3 Hz, 1H), 7.93 – 7.89 (m, 2H), 7.87 (d, *J* = 7.5 Hz, 1H), 7.76 (d, *J* = 9.1 Hz, 2H), 7.74 – 7.71 (m, 2H), 7.61 – 7.55 (m, 2H), 7.38 (td, *J* = 7.6, 1.0 Hz, 1H).^{13}C NMR (126 MHz, $CDCl_3$) δ 191.33, 145.69, 139.53, 138.44, 135.49, 131.74, 129.66, 129.43, 129.00, 127.02, 125.77, 124.01, 123.49, 123.26, 122.11, 119.88, 118.71, 118.67, 116.94, 116.62, 111.48, 93.82, 88.11. HRMS APCI, *m/z* calcd. for $C_{25}H_{14}NOS$: 376.0791, $[M+H]^+$; found: 376.0795.

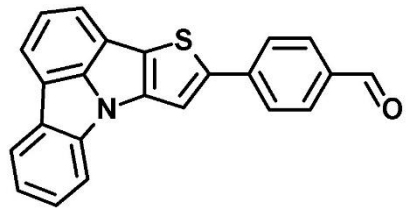

TPCz-ph-CHO - p-(thieno[2′,3′:4,5]pyrrolo[3,2,1-jk]carbazol-5-yl)benzaldehyde: In a round-bottom flask, equipped with a bubbler, septum, and condenser, 360 mg (0.95 mmol) of 5-iodo-thieno[2′,3′:4,5]pyrrolo[3,2,1-jk]carbazole and 1.2 eq. mol. (170 mg, 1.14 mmol) 4-formylphenylboronic acid were placed. Next, 14 mL of toluene and 7 mL of EtOH were added, and the mixture was stirred under argon for 30 min. After this time, 3 mL

of 2M Na_2CO_3 was added, and flushed by argon for next 5 min, and finally 90 mg (0.078 mmol) $[Pd(PPh_3)_4]$ was added. The mixture was stirred and heated at 90 °C for 24 h. After cooling, water was added and the organic phase was extracted with CHCl3. The organic layer was collected and dried over anhydrous MgSO4, and the crude product was purified by column chromatography on silica gel with dichloromethane:hexane (1:1) as eluent to give the product as a yellow solid state (300 mg, 0.85 mmol, yield = 90%). 1H NMR (500 MHz, CDCl3) δ 10.04 (s, 1H), 8.13 (dd, J = 7.7, 0.5 Hz, 1H), 7.98 (t, J = 5.4 Hz, 1H), 7.95 – 7.92 (m, 2H), 7.88 (dd, J = 6.7, 1.5 Hz, 2H), 7.86 (s, 1H), 7.84 (s, 1H), 7.80 (d, J = 8.0 Hz, 1H), 7.60 – 7.54 (m, 2H), 7.38 (td, J = 7.6, 0.9 Hz, 1H). 13C NMR (126 MHz, DMSO) δ 192.70, 144.95, 144.54, 141.69, 140.41, 138.29, 135.68, 131.06, 129.13, 127.80, 125.81, 124.20, 123.89, 122.81, 119.68, 119.36, 117.19, 112.75, 111.99. HRMS ESI m/z calcd. For C23H14NOS: 352.0796 [M+H]+; found: 352.0773.

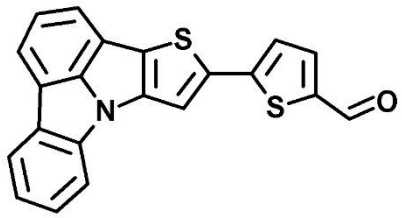

TPCz-th-CHO - 5-(thieno[2′,3′:4,5]pyrrolo[3,2,1-jk]carbazol-5-yl)thiophene-2-carboxaldehyde: The procedure for obtaining it was the same as for TPCz-ph-CHO, only using the 5-formyl-2-thiopheneboronic acid as a substrate. The product was eluted on silica with dichloromethane:hexane (1:1) as eluent to give the product as an orange solid state (206 mg, 0.58 mmol, yield = 43%). ^{1}H NMR (500 MHz, $CDCl_3$) δ 9.92 (s, 1H), 8.13 (d, *J* = 7.6 Hz, 1H), 7.99 (d, *J* = 7.2 Hz, 1H), 7.86 (d, *J* = 7.6 Hz, 1H), 7.81 (dt, *J* = 7.9, 0.9 Hz, 1H), 7.76 (s, 1H), 7.74 (d, *J* = 4.0 Hz, 1H), 7.61 – 7.55 (m, 2H), 7.41 (d, *J* = 4.0 Hz, 1H), 7.39 (td, *J* = 7.6, 1.0 Hz, 1H). ^{13}C NMR (126 MHz, $CDCl_3$) δ 182.29, 147.82, 145.10, 141.79, 140.71, 138.39, 137.83, 137.24, 129.47, 127.03, 124.75, 123.95, 123.56, 123.21, 122.16, 119.91, 118.60, 118.56, 116.91, 111.59, 110.03. HRMS ESI $[M+H]^+$ *m/z* calcd. for C21H12NOS2: 358.0360, $[M+H]^+$; found: 358.0341.

NMR Spectra

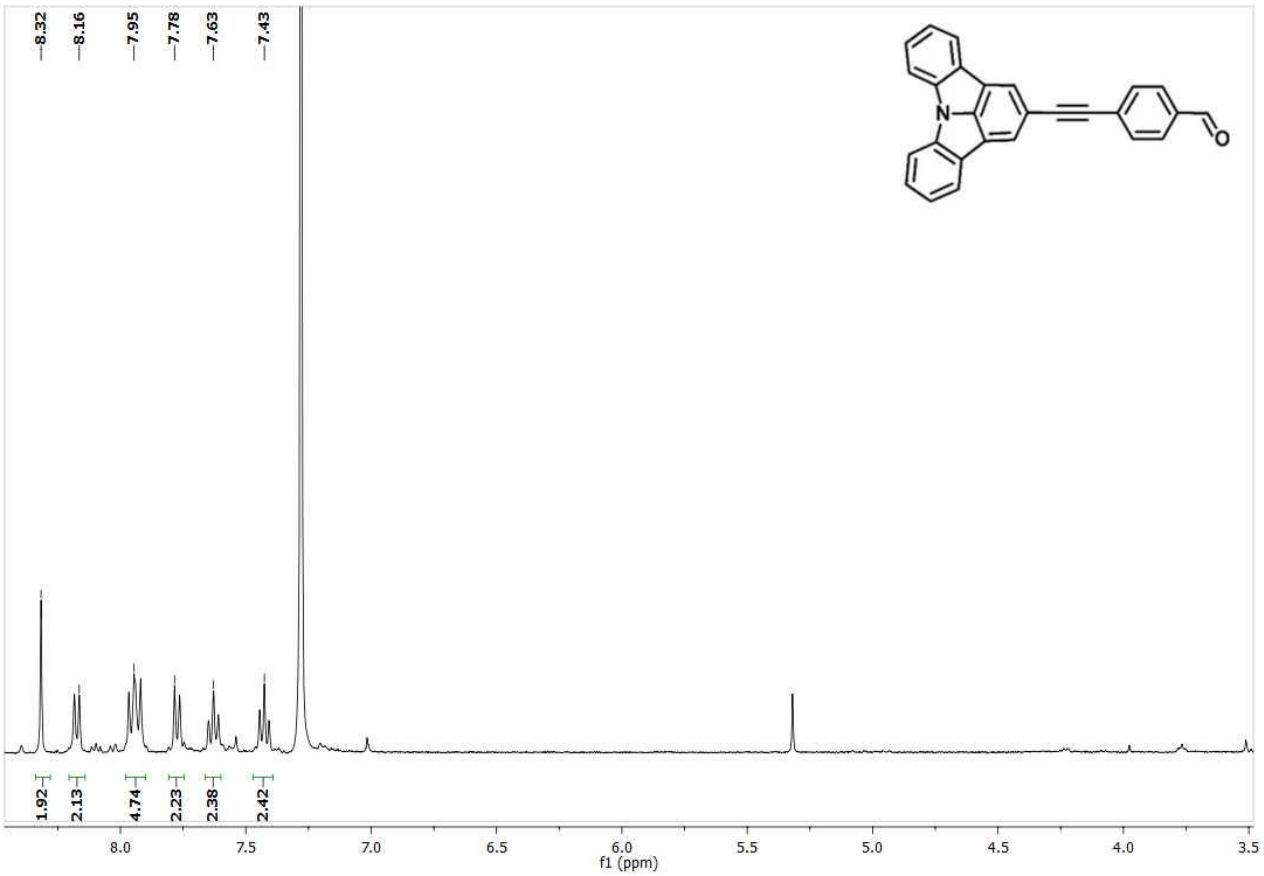
8.32
8.16
7.95
7.78
7.63
7.43
1.92
2.13
4.74
2.23
2.38
2.42
f1 (ppm)

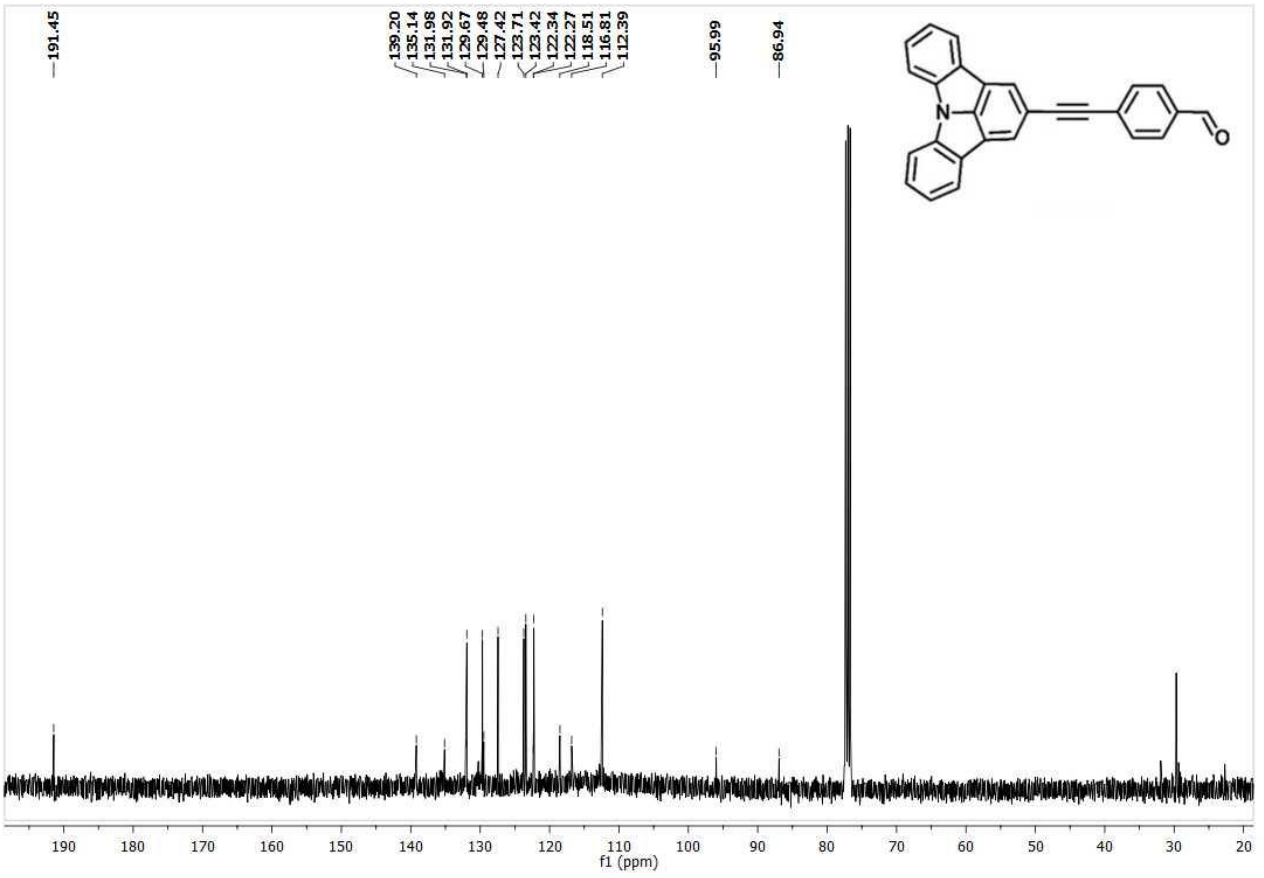
191.45
139.20
135.14
131.98
131.92
129.67
129.48
127.42
123.71
123.42
122.34
122.27
118.51
116.81
112.39
95.99
86.94
f1 (ppm)

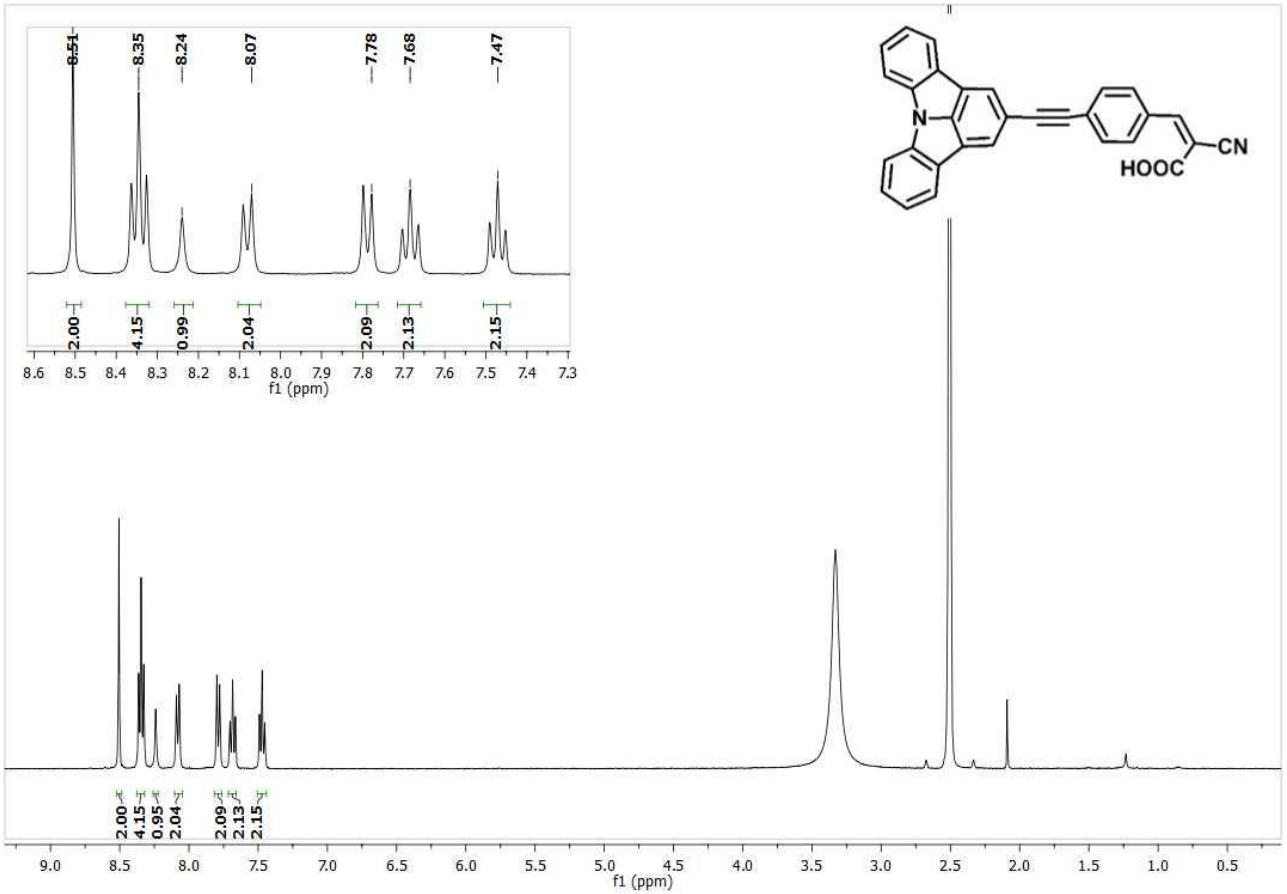
8.51
8.35
8.24
8.07
7.78
7.68
7.47
2.00
4.15
0.99
2.04
2.09
2.13
2.15
f1 (ppm)
N
HOOC
CN

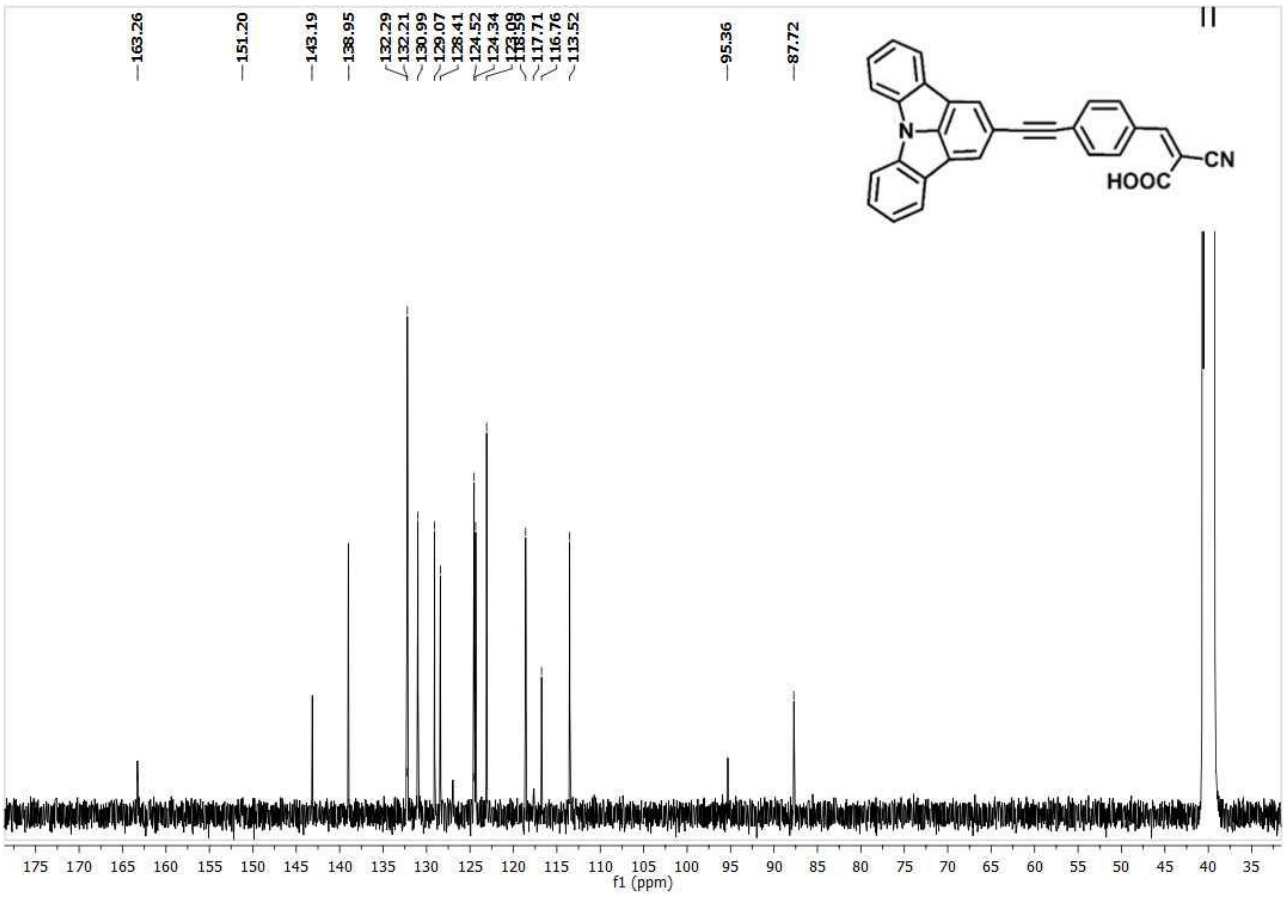
163.26
151.20
143.19
138.95
132.29
132.21
130.99
129.07
128.41
124.52
124.34
118.59
117.71
116.76
113.52
95.36
87.72
f1 (ppm)
N
HOOC
CN

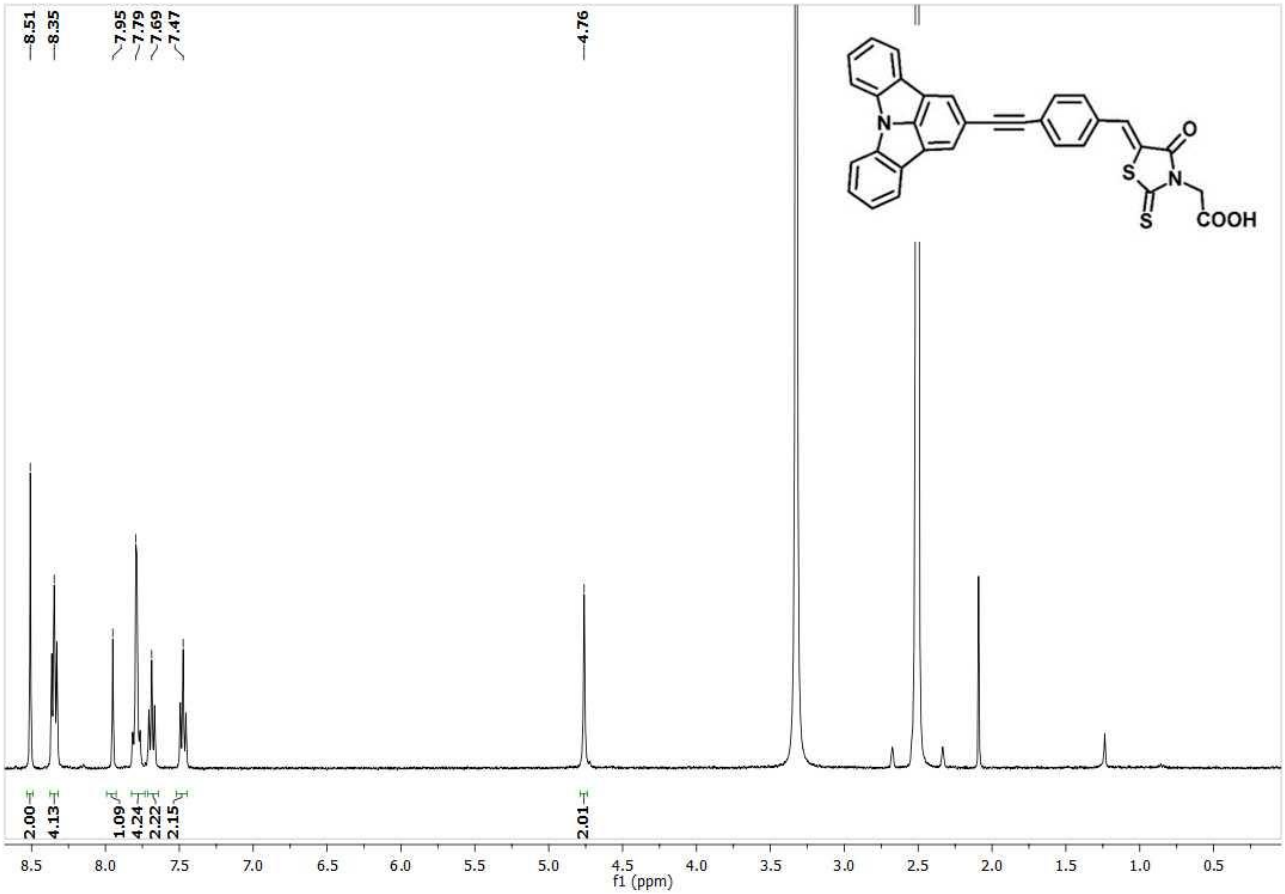
8.51
8.35
7.95
7.79
7.69
7.47
4.76
2.00
4.13
1.09
4.24
2.22
2.15
2.01
f1 (ppm)
N
O
S
N
S
COOH

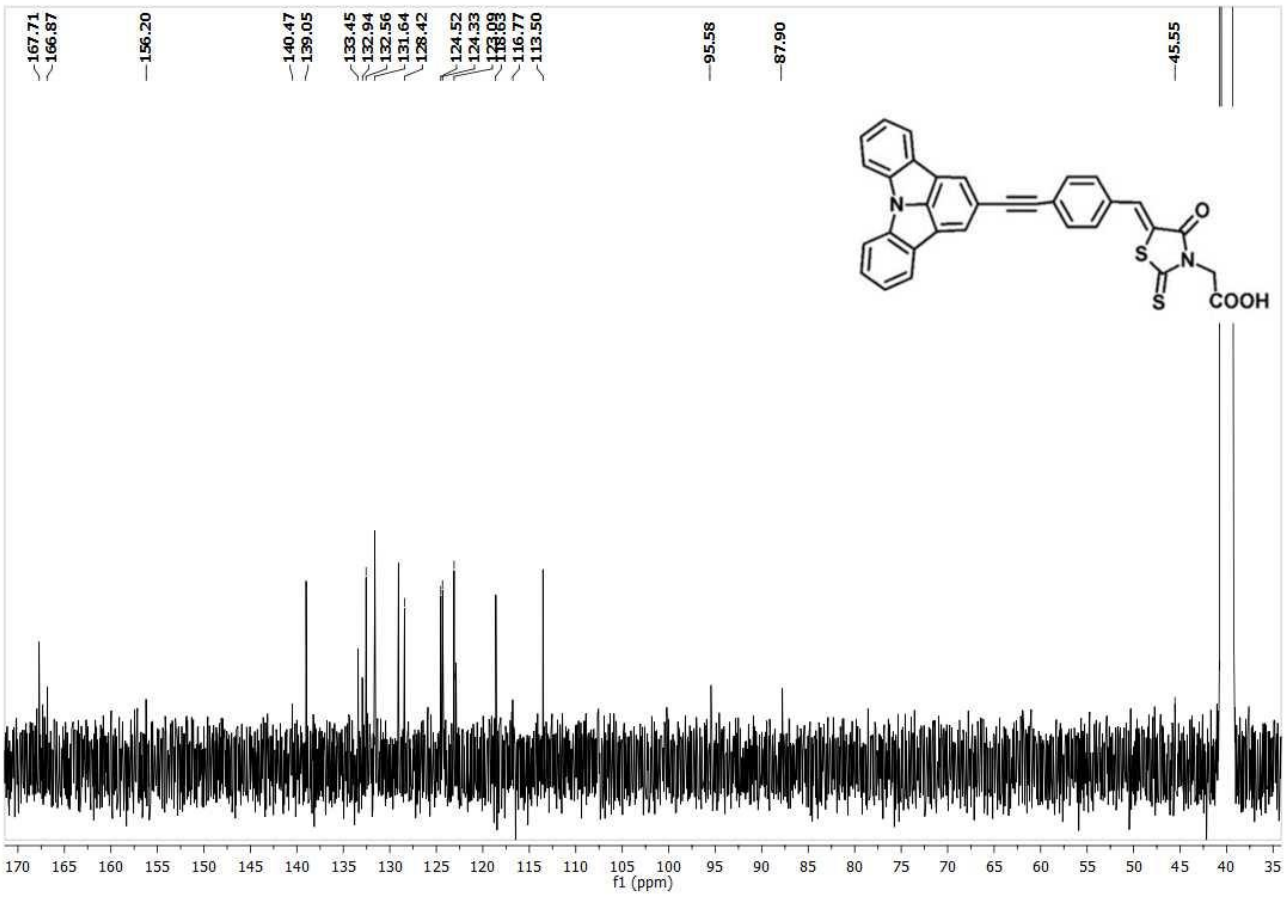
167.71
166.87
156.20
140.47
139.05
133.45
132.94
132.56
131.64
128.42
124.52
124.33
116.77
113.50
95.58
87.90
45.55
f1 (ppm)
N
O
S
N
S
COOH

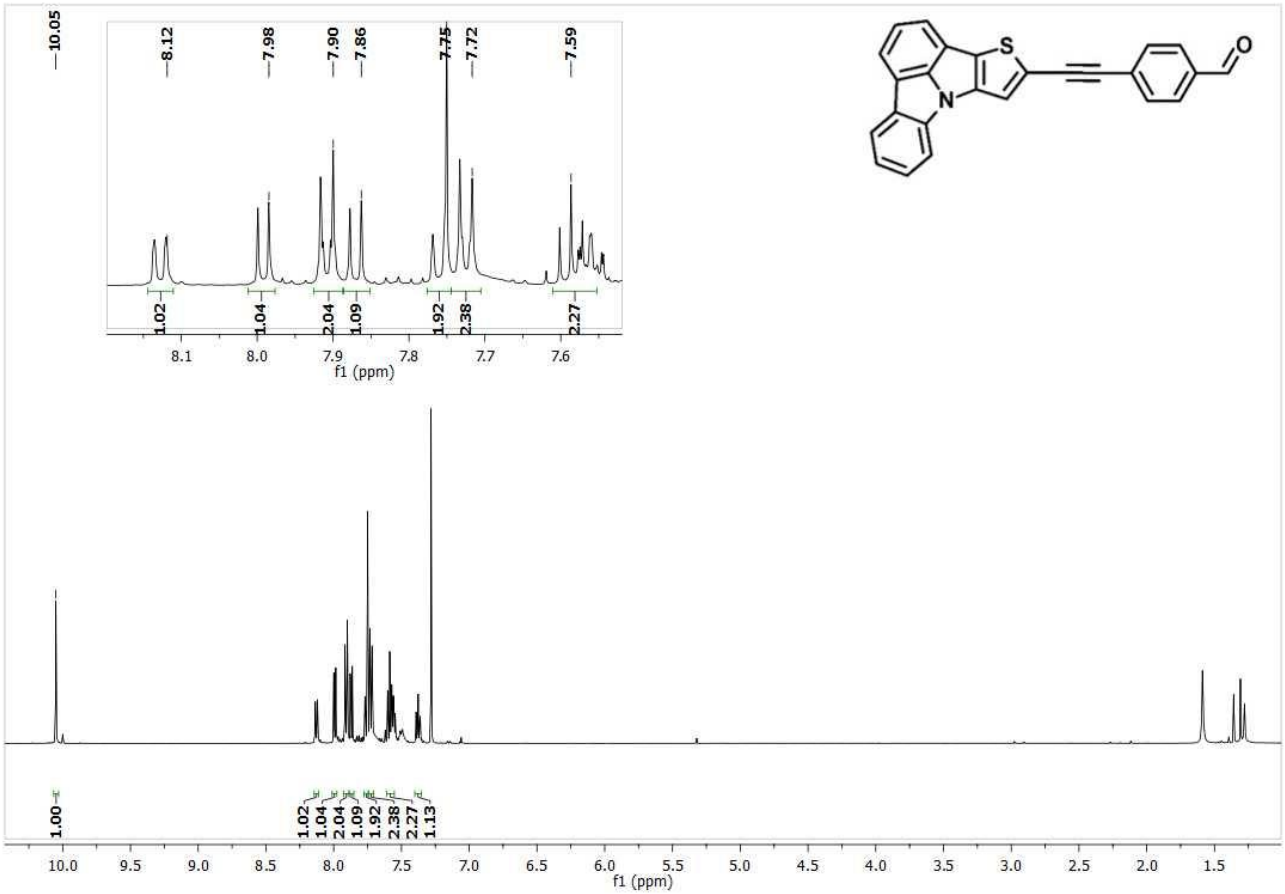
10.05
8.12
7.98
7.90
7.86
7.75
7.72
7.59
1.02
1.04
2.04
1.09
1.92
2.38
2.27
f1 (ppm)
1.00
1.02
1.04
2.04
1.09
1.92
2.38
2.27
1.13
f1 (ppm)
S
N
O

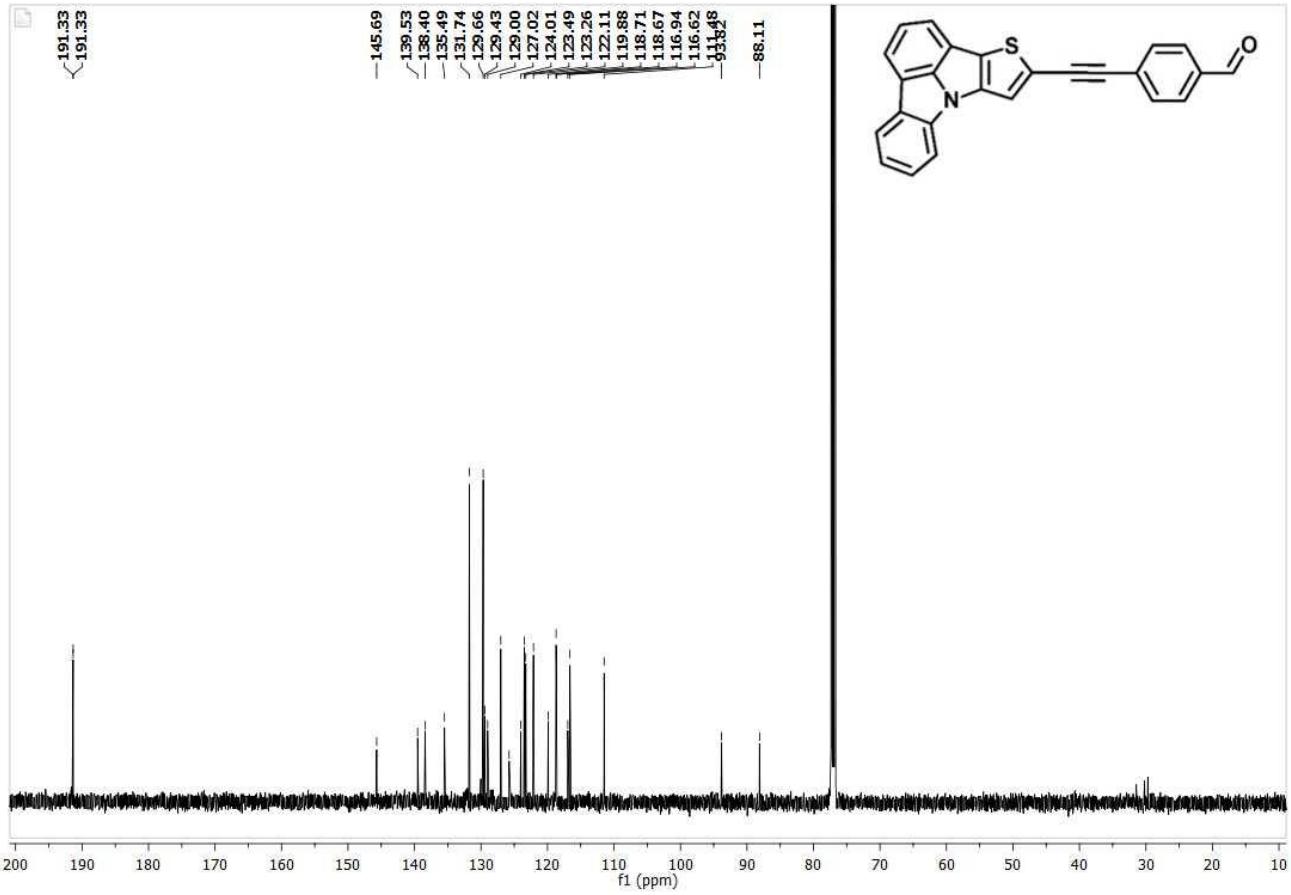
191.33
191.33
145.69
139.53
138.40
135.49
131.74
129.66
129.43
129.00
127.02
124.01
123.49
123.26
122.11
119.88
118.71
118.67
116.94
116.62
111.48
93.82
88.11
f1 (ppm)
S
N
O

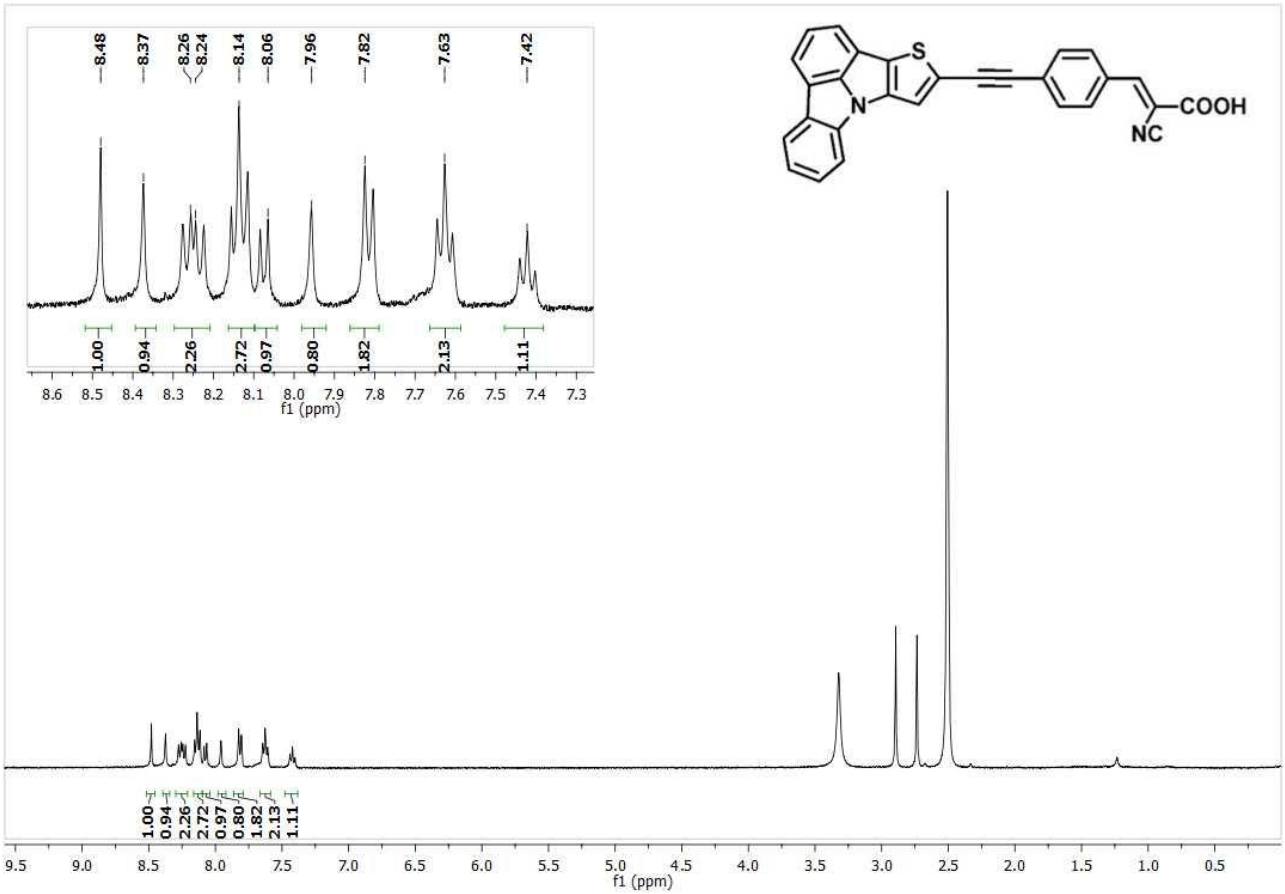
8.48
8.37
8.26
8.24
8.14
8.06
7.96
7.82
7.63
7.42
1.00
0.94
2.26
2.72
0.97
0.80
1.82
2.13
1.11
f1 (ppm)
S
N
COOH
NC

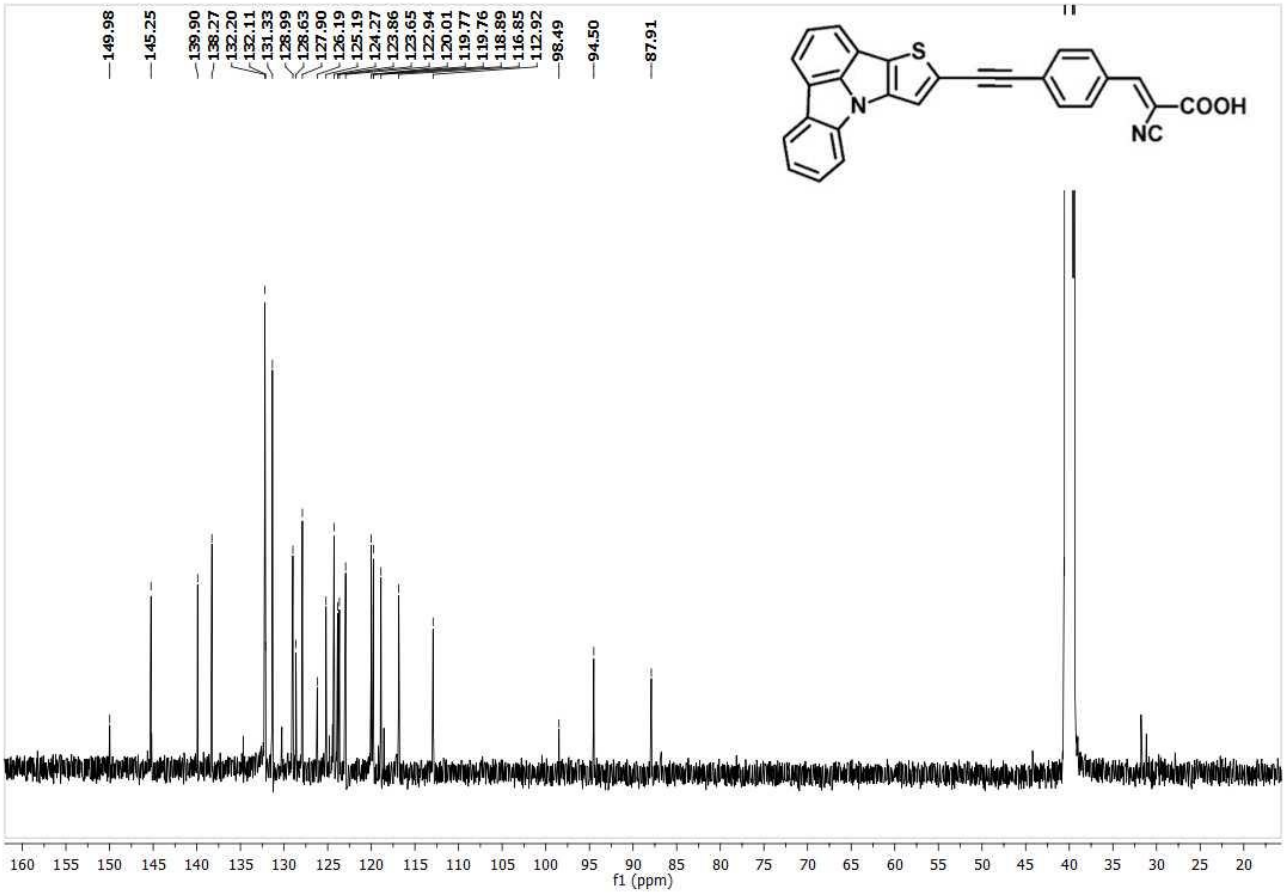
149.98
145.25
139.90
138.27
132.20
132.11
131.33
128.99
128.63
127.90
126.19
125.19
124.27
123.86
123.65
122.94
120.01
119.77
119.76
118.89
116.85
112.92
98.49
94.50
87.91
f1 (ppm)
S
N
COOH
NC

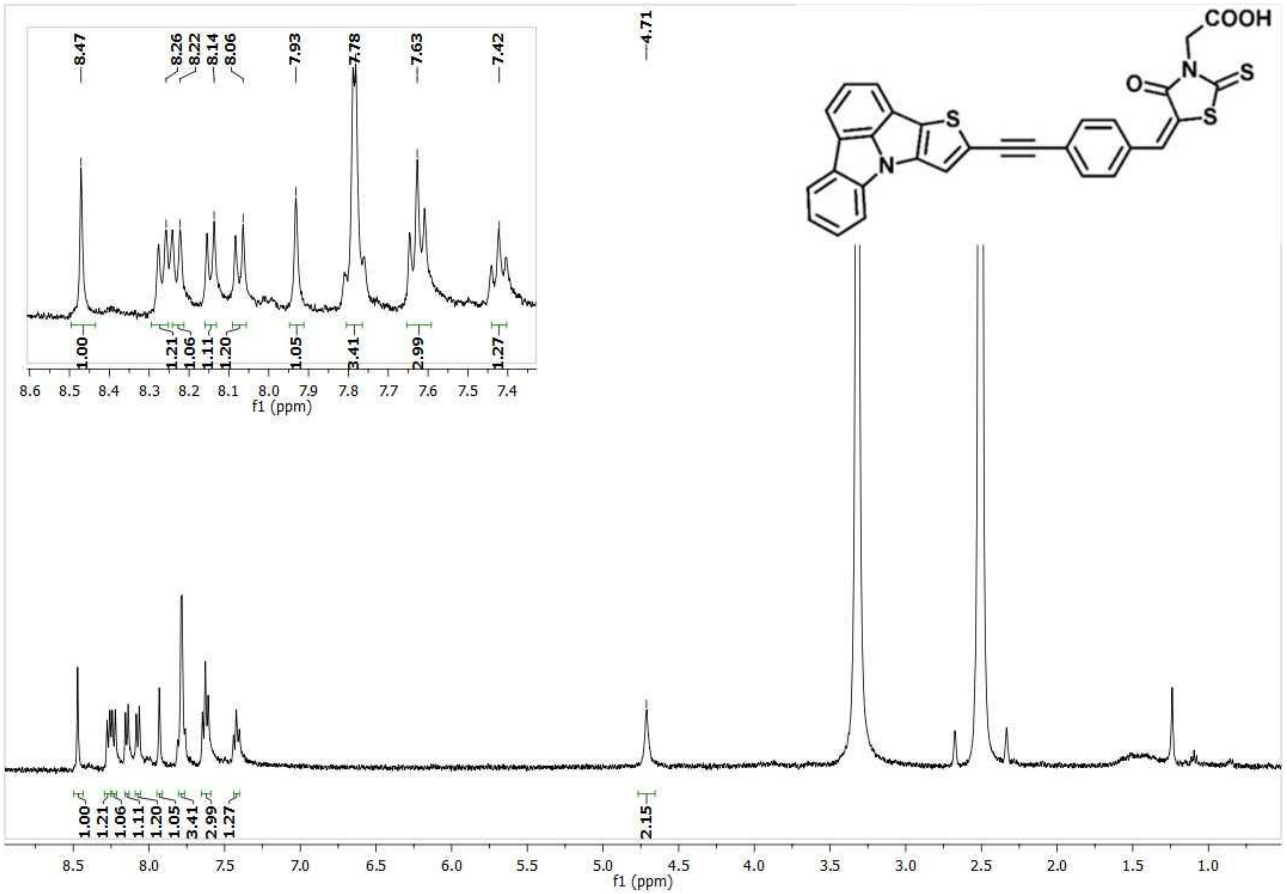
8.47
8.26
8.22
8.14
8.06
7.93
7.78
7.63
7.42
4.71
COOH
N
O
S
S
S
N
1.00
1.21
1.06
1.11
1.20
1.05
3.41
2.99
1.27
2.15
f1 (ppm)

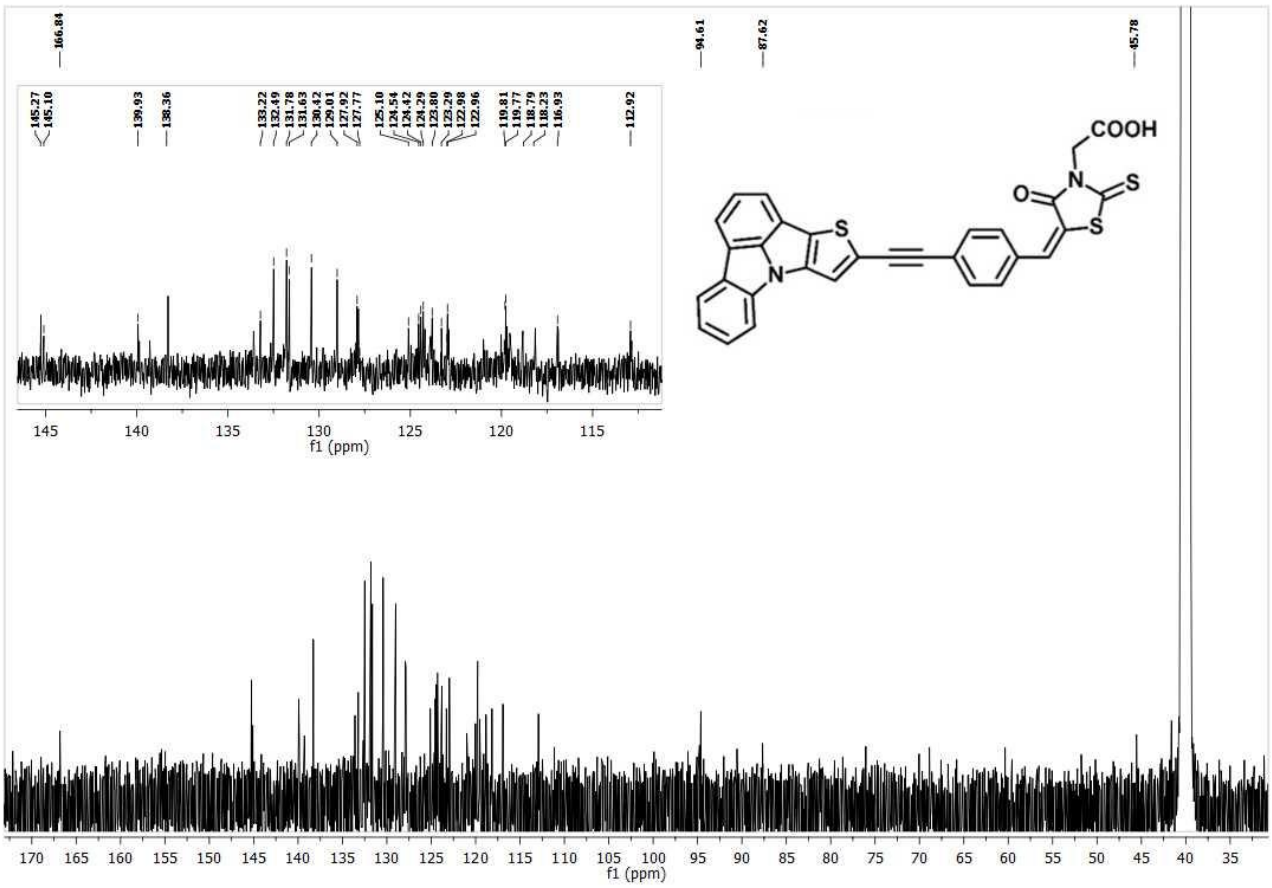
166.84
94.61
87.62
45.78
145.27
145.10
130.93
128.36
133.22
132.49
131.78
131.63
130.42
129.01
127.92
127.77
125.10
124.54
124.22
124.20
123.80
123.29
122.98
122.96
119.81
119.77
118.79
118.23
116.93
112.92
COOH
N
O
S
S
S
N
f1 (ppm)

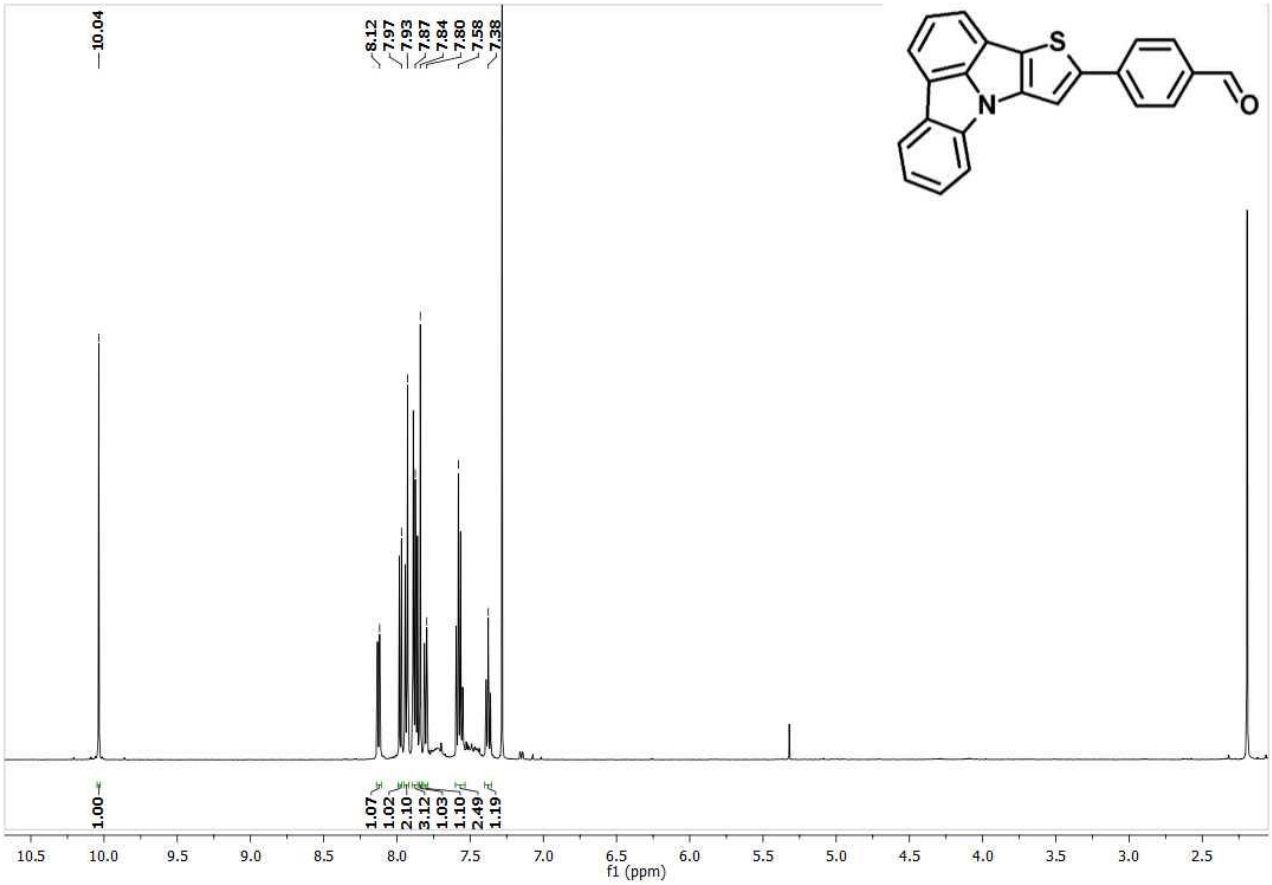
10.04
8.12
7.97
7.93
7.87
7.84
7.80
7.58
7.38
1.00
1.07
1.02
2.10
3.12
1.03
1.10
2.49
1.19
f1 (ppm)

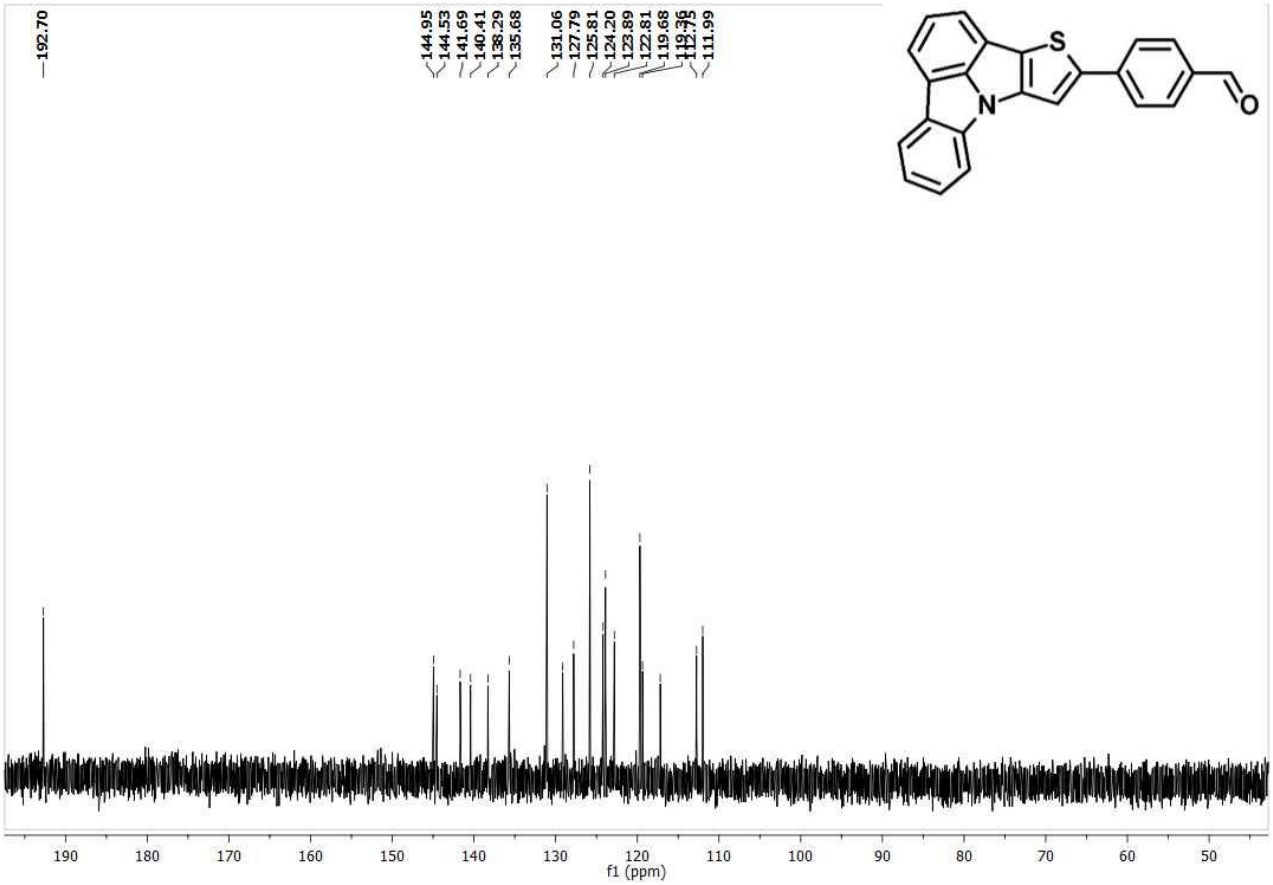
192.70
144.95
144.53
141.69
140.41
138.29
135.68
131.06
127.79
125.81
124.20
123.89
122.81
119.68
111.99
f1 (ppm)

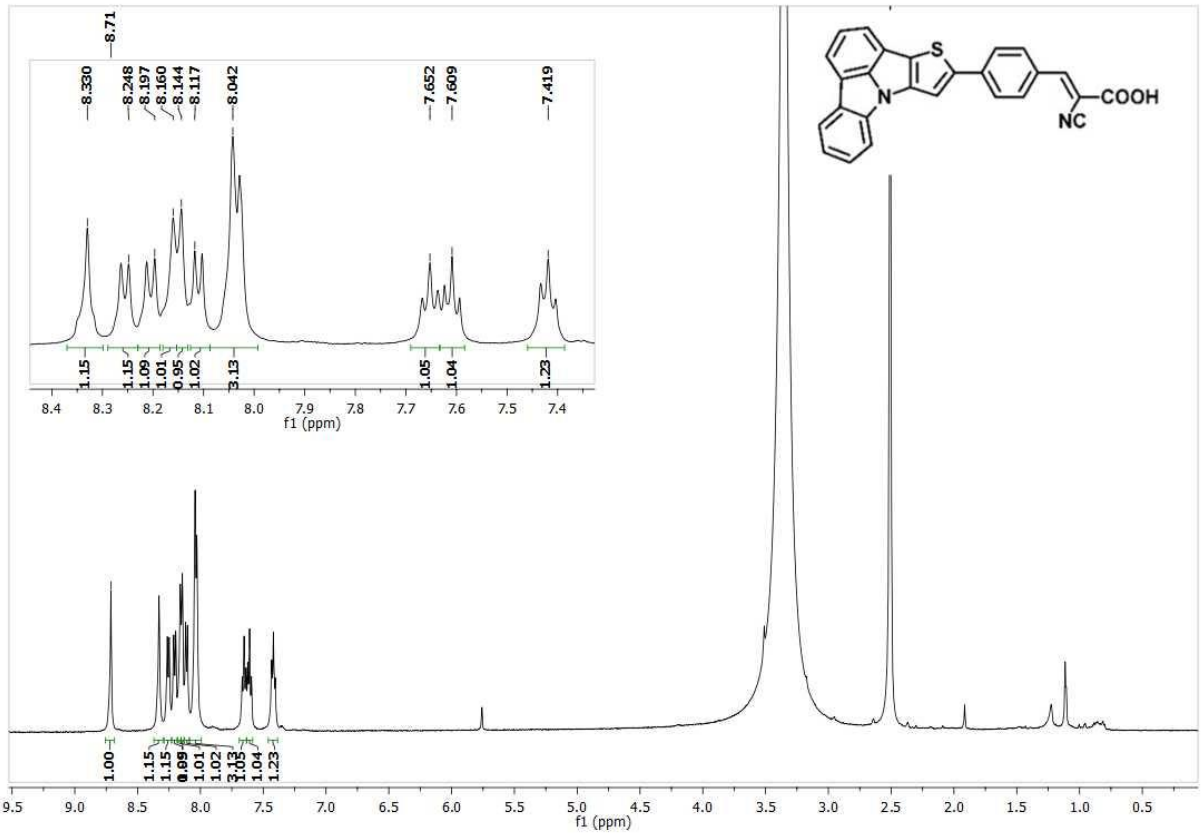
8.71
8.330
8.248
8.197
8.160
8.144
8.117
8.042
7.652
7.609
7.419
1.15
1.15
1.09
1.01
0.95
1.02
3.13
1.05
1.04
1.23
f1 (ppm)
S
N
COOH
NC

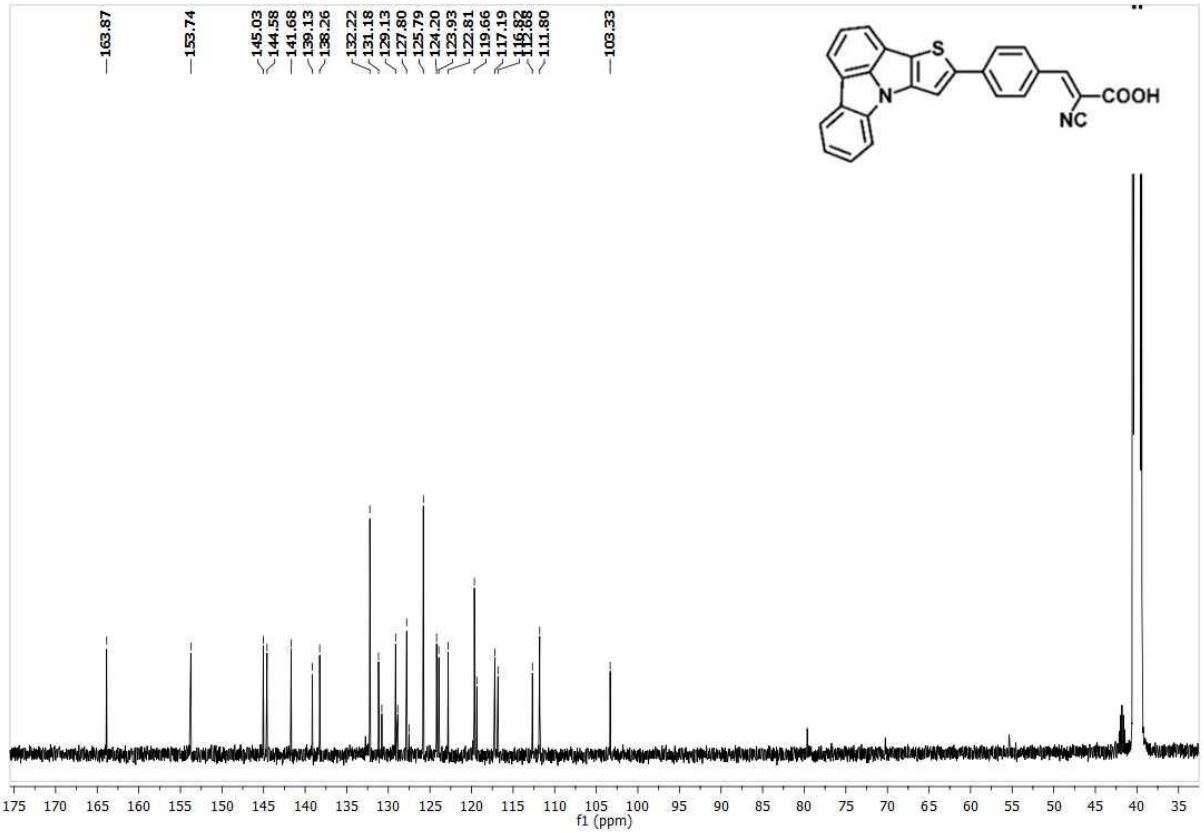
163.87
153.74
145.03
144.58
141.68
139.13
138.26
132.22
131.18
129.13
127.80
125.79
124.20
123.93
122.81
119.66
117.19
111.80
103.33
f1 (ppm)
S
N
COOH
NC

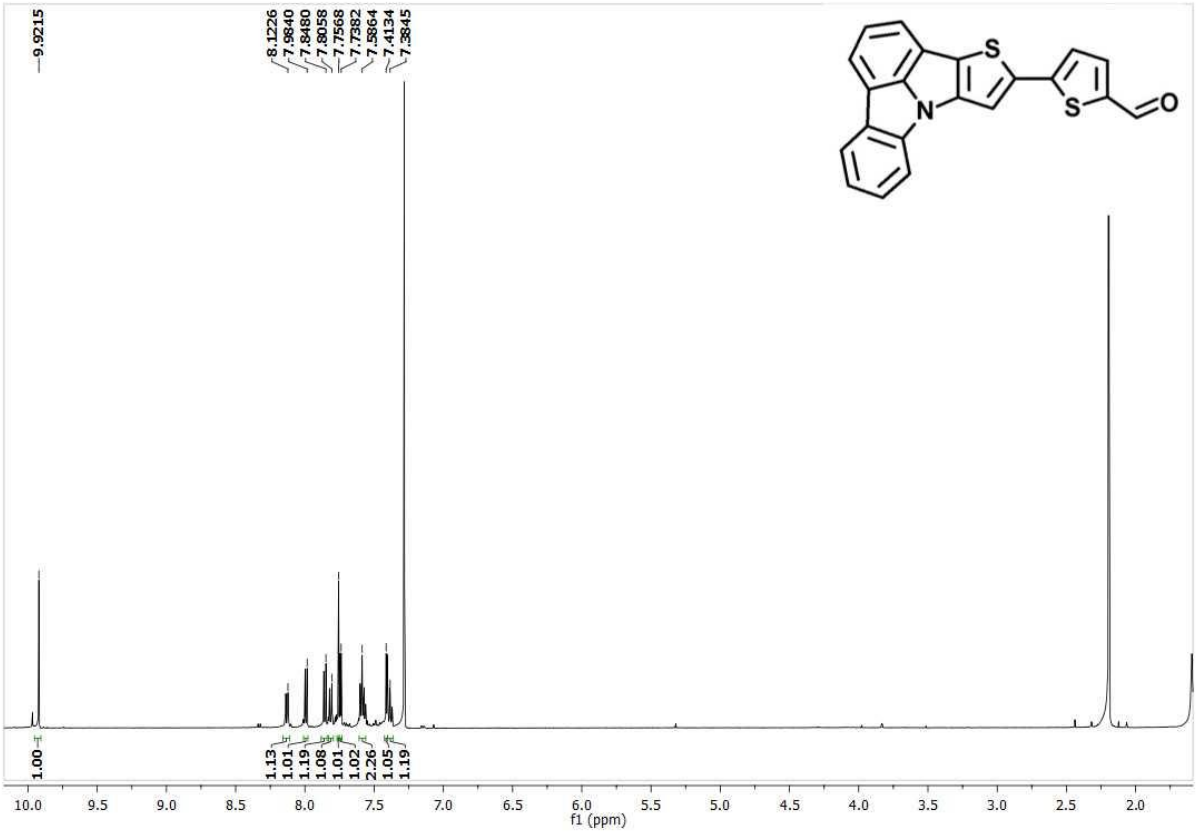
9.9215
8.1226
7.9840
7.8480
7.8058
7.7568
7.7382
7.5864
7.4134
7.3845
1.00
1.13
1.01
1.19
1.08
1.01
1.02
2.26
1.05
1.19
S
N
S
O
f1 (ppm)

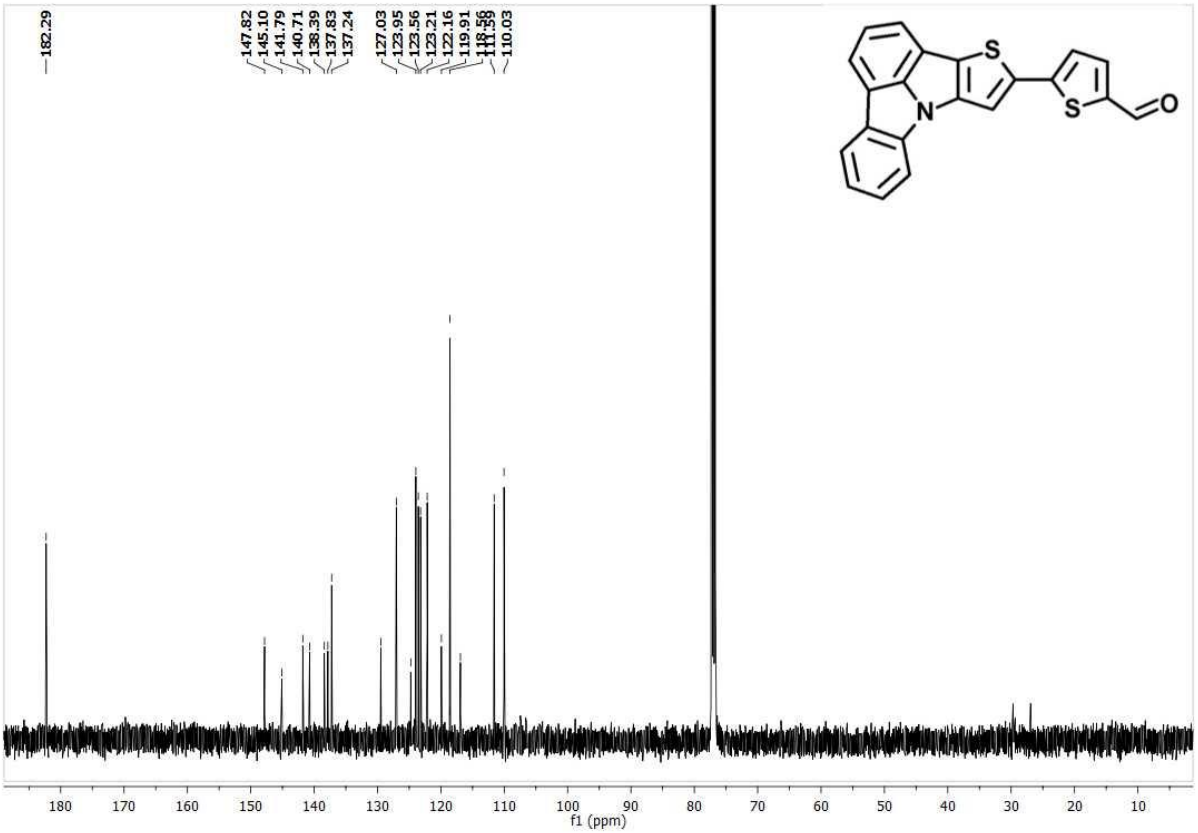
182.29
147.82
145.10
141.79
140.71
138.39
137.83
137.24
127.03
123.95
123.56
123.21
122.16
119.91
110.03
S
N
S
O
f1 (ppm)

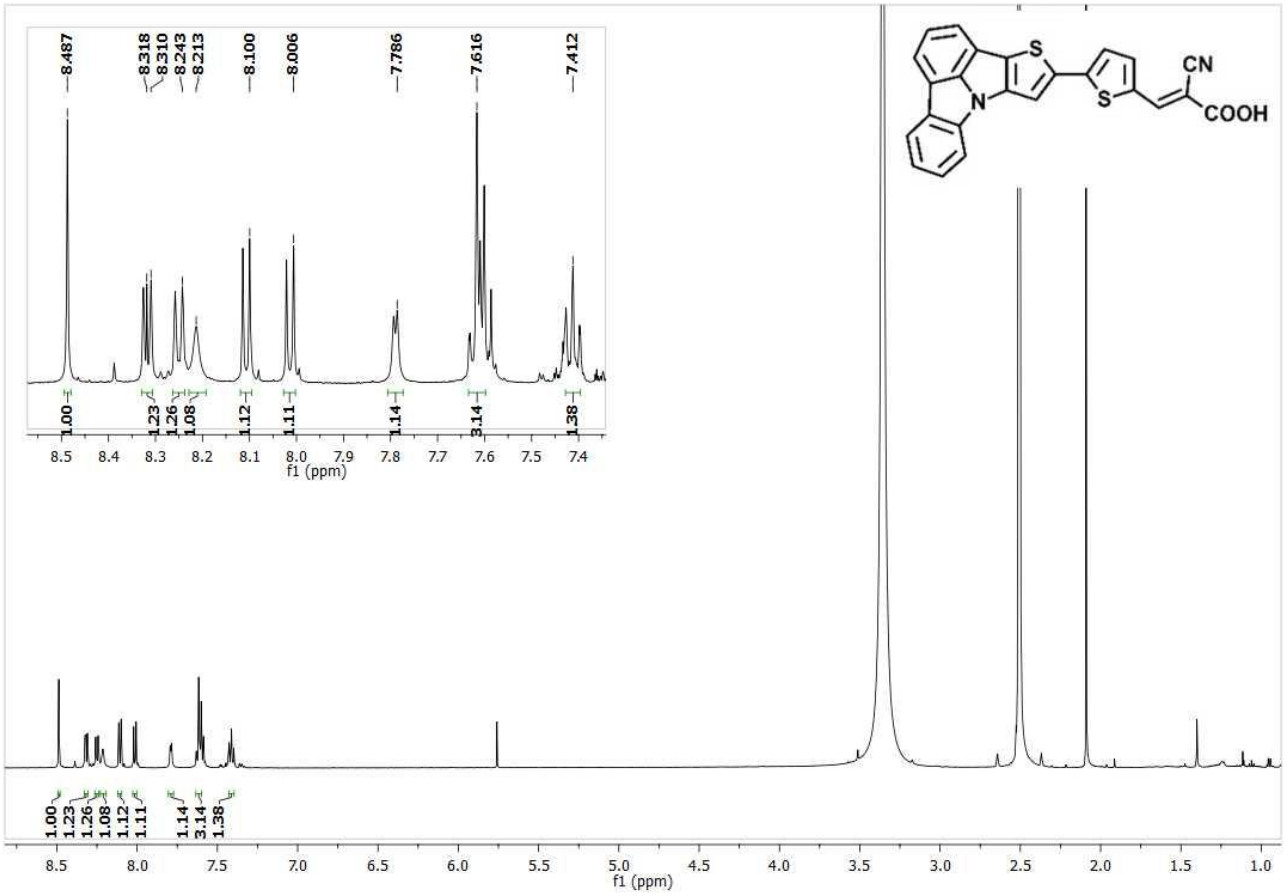
8.487
8.318
8.310
8.243
8.213
8.100
8.006
7.786
7.616
7.412
1.00
1.23
1.26
1.08
1.12
1.11
1.14
3.14
1.38
f1 (ppm)
S
N
S
CN
COOH

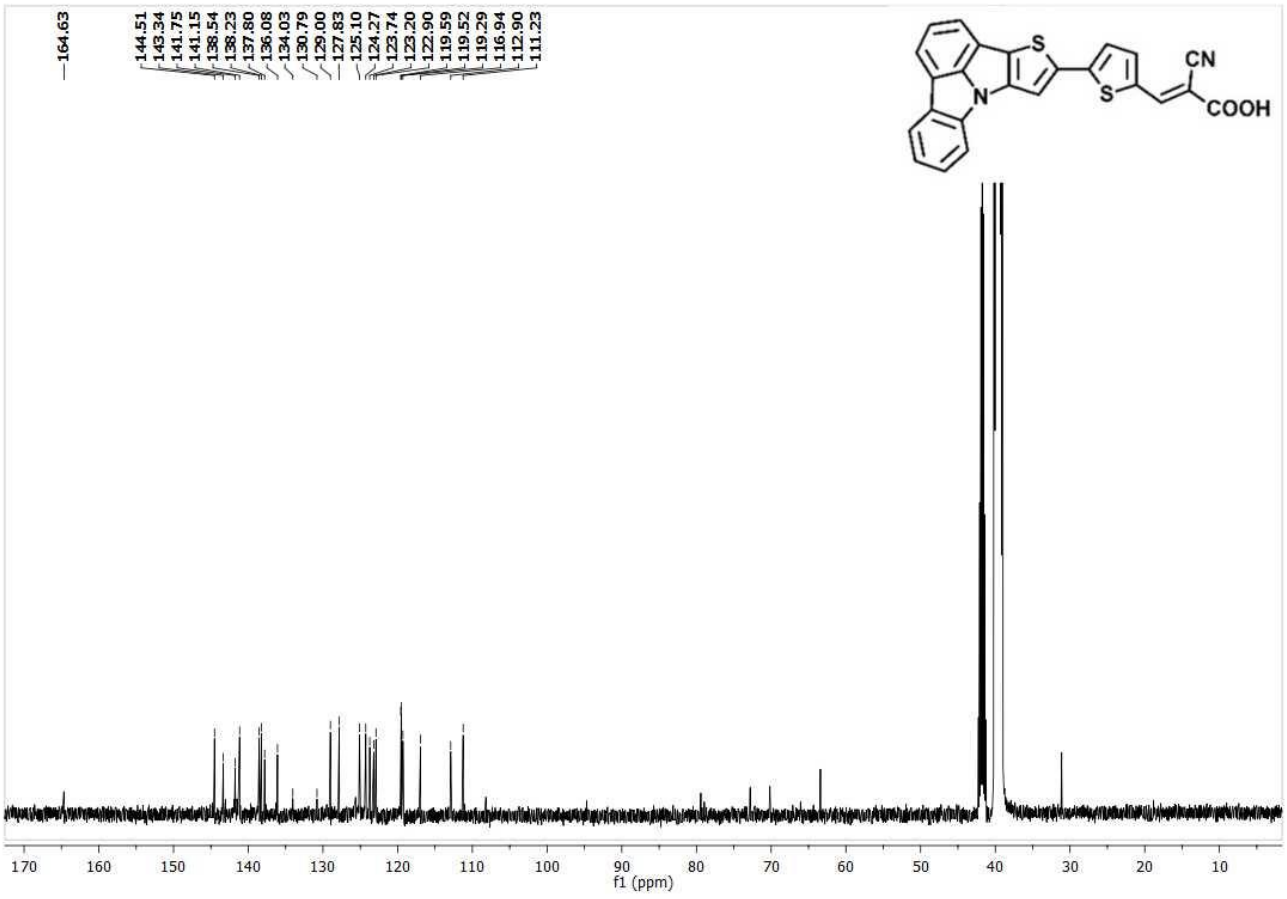
164.63
144.51
143.34
141.75
141.15
138.54
138.23
137.80
136.08
134.03
130.79
129.00
127.83
125.10
124.27
123.74
123.20
122.90
119.59
119.52
119.29
116.94
112.90
111.23
f1 (ppm)
S
N
S
CN
COOH

Thermal measurements

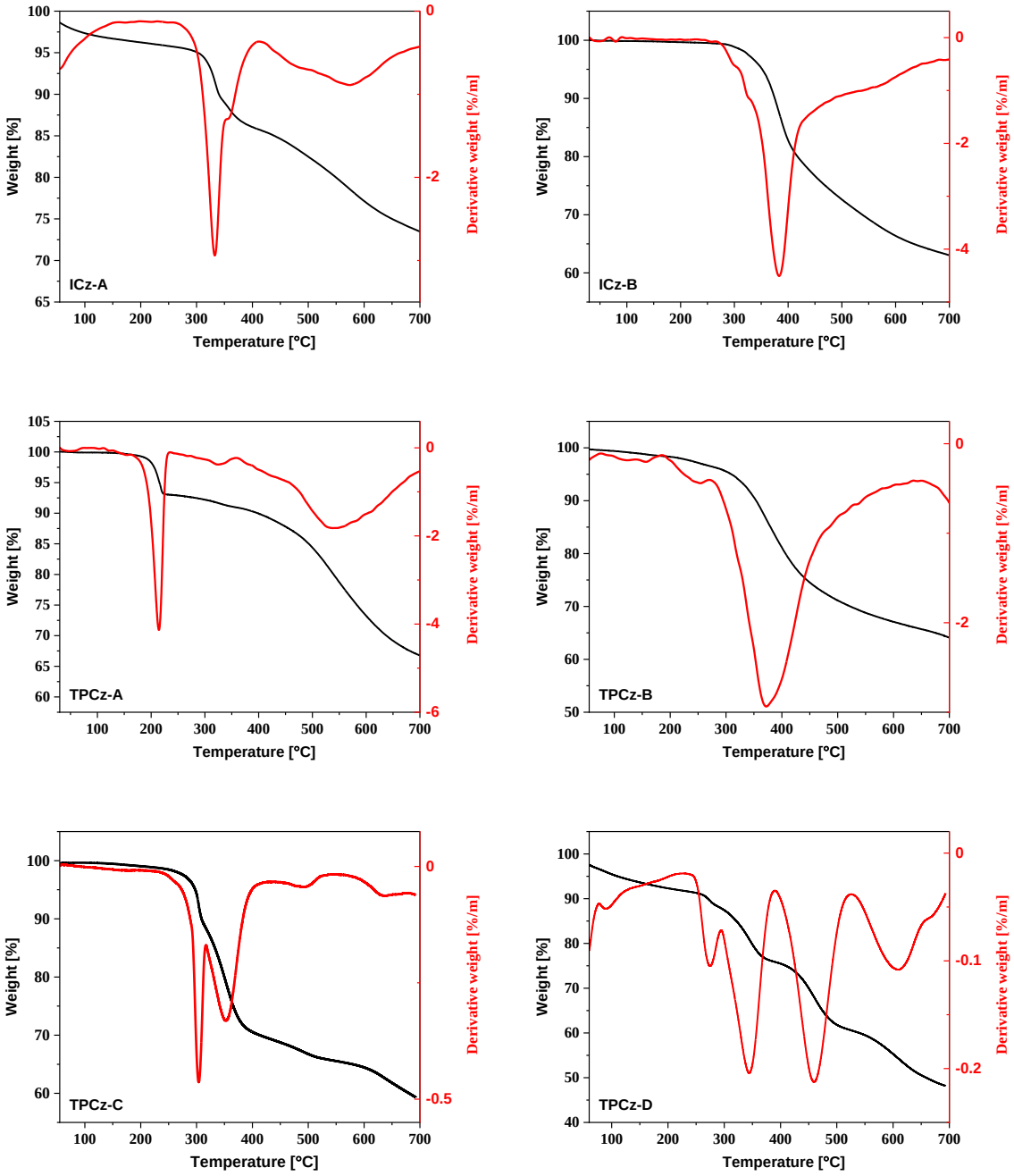

Fig. S1. Thermogravimetric analysis of **ICz-A** – **TPCz-D**.

Table S1. Thermal characteristics of **ICz-A** – **TPCz-D**.

Compound	T_5 (°C)	T_{10} (°C)	T_{max} (°C)	Char residue at 700 °C
ICz-A	301	339	332	73
ICz-B	352	375	382	63
TPCz-A	214	353	215	66
TPCz-B	310	354	372	64
TPCz-C	297	309	303; 352	59
TPCz-D	106	270	273; 344; 458; 605	48

Theoretical calculations

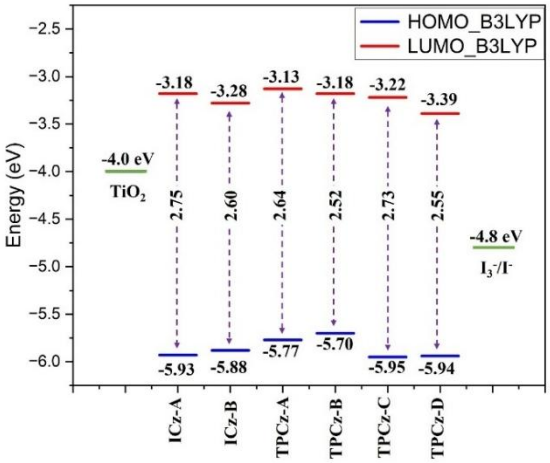

Fig. S2. Diagram of the HOMO and LUMO energies levels (eV), with the calculated E_{gap}, obtained by B3LYP/6-31G(d) method in DCM media of the studied dyes.

Table S2. Calculated by TD-DFT (CAM-B3LYP/LANL2DZ;6-31G(d,p)), the lowest energy absorption bands with oscillator strengths and LHE for complex systems dye@TiO2.

Compound CAM-B3LYP	Absorption [nm] (oscillator strengths)	Transitions	LHE
ICz-A@TiO_2	378.46 (1.9699)	HOMO→LUMO+3(15%); HOMO→LUMO+5(13%)	0.99
ICz-B@TiO_2	398.01 (2.0685)	HOMO→LUMO+5(28%)	0.99
TPCz-A@TiO_2	400.87 (2.0801)	HOMO→LUMO+3 (25%)	0.99
TPCz-B@TiO_2	413.17 (2.2019)	HOMO→LUMO+3 (36%)	0.99
TPCz-C@TiO_2	392.07 (1.6042)	HOMO→LUMO+3 (22%); HOMO→LUMO+5 (10%)	0.97
TPCz-D@TiO_2	441.31 (1.2709)	HOMO→LUMO+1 (10%); HOMO→LUMO+3 (29)	0.94

Table S3. Natural transition orbitals (NTOs) showing the hole (occupied) and particle (unoccupied) pairs for the lowest-energy electronic transitions of **ICz-A**–**TPCz-D**, calculated at the CAM-B3LYP/6-311G(d,p) level in DCM.

dye	Hole	Particle
ICz-A 360.38 (1.782)	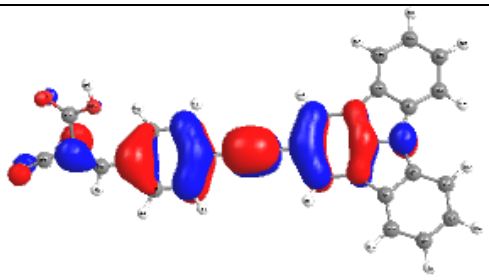	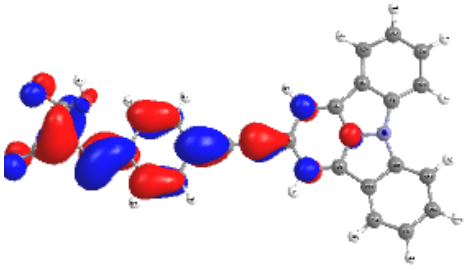
ICz-B **399.6** **(2.051)**	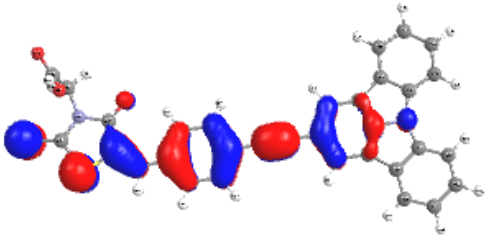	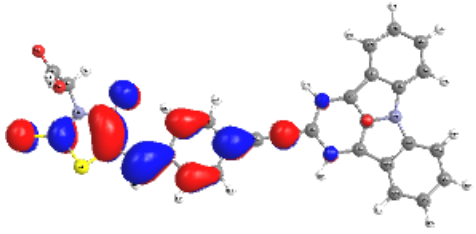
TPCz-A 385.43 (1.881)	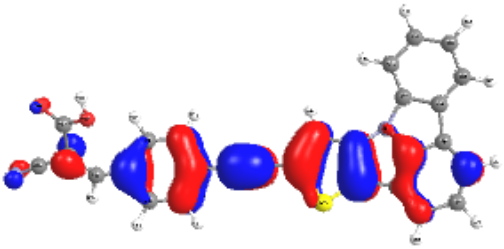	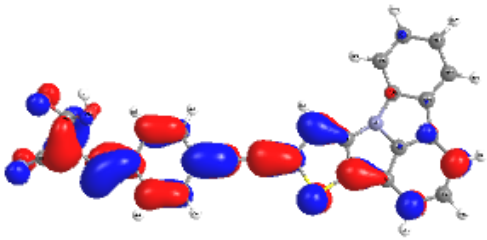
TPCz-B 415.28 (2.279)	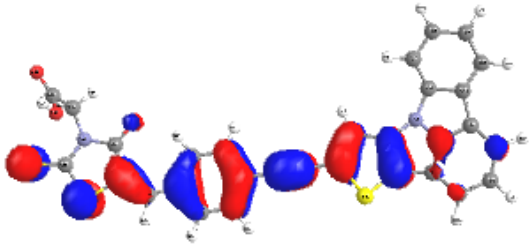	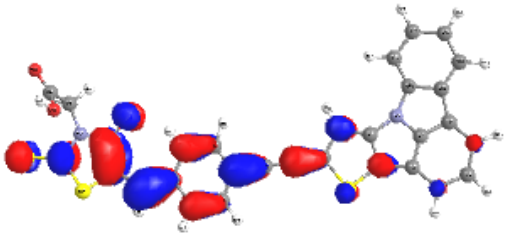
TPCz-C 381.41 (1.460)	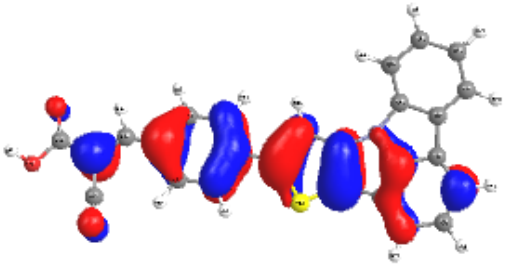	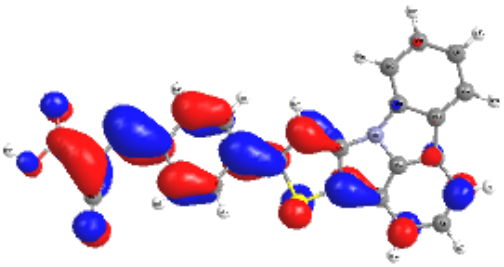
TPCz-D 425.16 (1.5270)	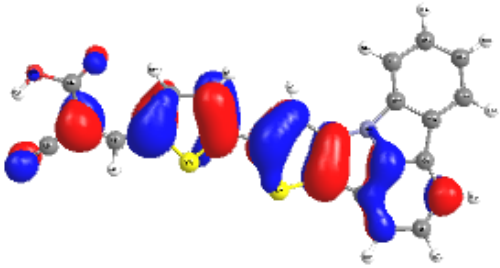	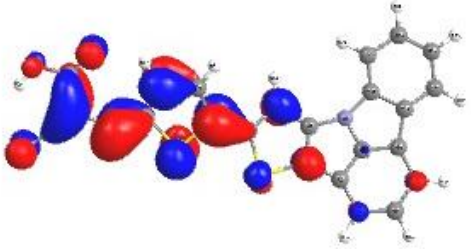

Table S4. The optimised structures (CAM-B3LYP/6-311G(d,p) in DCM) of **ICz-A** – **TPCz-D** with contours (0.025) of selected orbitals (HOMO, LUMO) and their energies with the contribution of the individual parts of the molecules in their creation (core/ring/acetylene bridge/anchoring group)

dye	% HOMO	HOMO [eV]	LUMO [eV]	% LUMO	ΔE [eV]
ICz-A	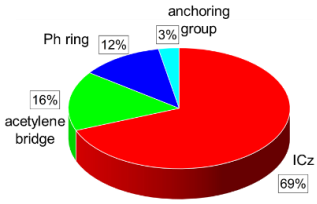	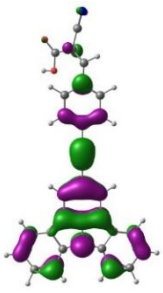 -6.77	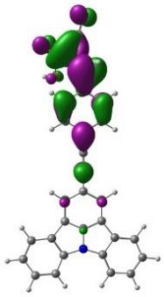 -1.47	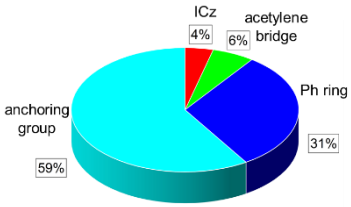	5.3
ICz-B	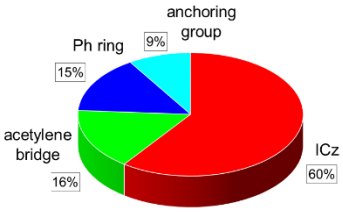	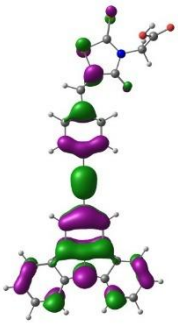 -6.71	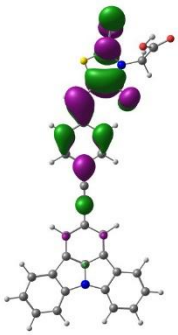 -1.72	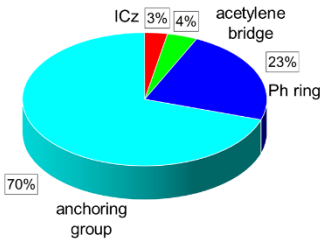	4.99
TPCz-A	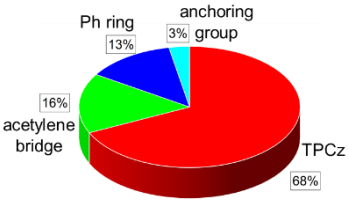	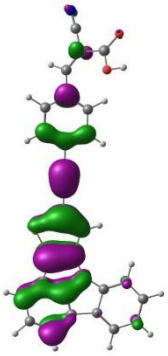 -6.77	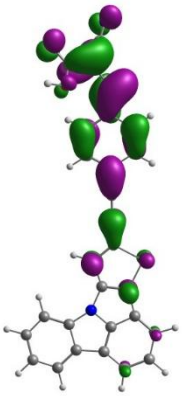 -1.59	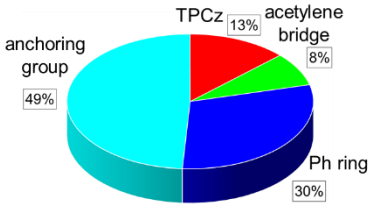	5.18
TPCz-B	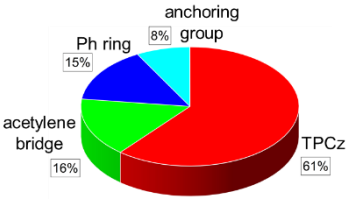	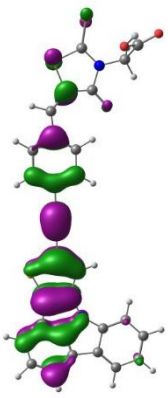 -6.71	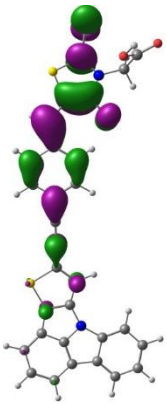 -1.82	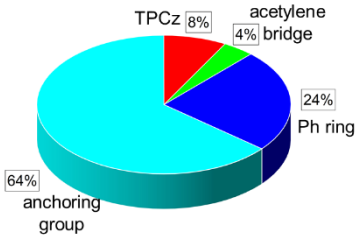	4.89

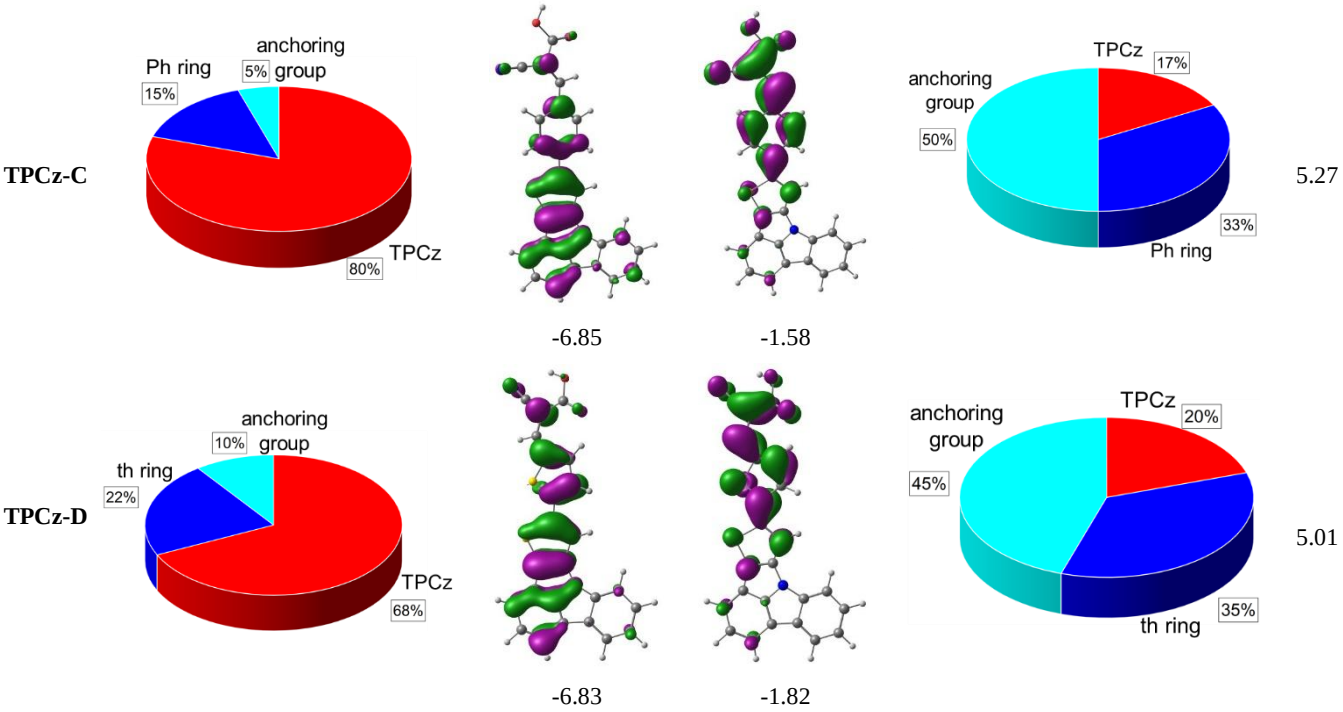

Table S5. TD-DFT calculated (6-311G(d,p)/CAM-B3LYP, DCM) absorption wavelength for **ICz-A** – **TPCz-D**.

Compound	Absorption [nm] (oscillator strengths)	Transitions
ICz-A	360.38 (1.7817)	HOMO →LUMO (35%)
	310.96 (0.1837)	HOMO →LUMO+1 (41%)
	272.43 (0.0346)	HOMO-3 →LUMO (11%) HOMO-1 →LUMO (11%)
	270.02 (0.0254)	HOMO-5 →LUMO (39%)
	253.97 (0.2612)	HOMO-2 →LUMO+1 (13%) HOMO-1 →LUMO (9%)
ICz-B	399.67 (2.0510)	HOMO →LUMO (33%)
	311.38 (0.1792)	HOMO →LUMO+1 (38%)
	307.79 (0.0786)	HOMO-3 →LUMO (19%)
	268.43 (0.1503)	HOMO-1 →LUMO (22%)
	258.08 (0.2625)	HOMO-8 →LUMO (33%)
TPCz-A	385.43 (1.8812)	HOMO →LUMO (37%)
	319.04 (0.2792)	HOMO-1 →LUMO (19%) HOMO-1 →LUMO+1 (19%)
	303.46 (0.0476)	HOMO →LUMO+1 (24%)
	276.67 (0.1205)	HOMO-2 →LUMO (16%) HOMO-2 →LUMO+1 (21%)
	270.19 (0.0445)	HOMO-5 →LUMO (18%)
	258.86 (0.1639)	HOMO-3 →LUMO (17%)
TPCz-B	415.28 (2.2791)	HOMO →LUMO (36%)
	317.96 (0.3087)	HOMO-1 →LUMO (15%) HOMO-1 →LUMO+1 (22%)
	279.17 (0.1572)	HOMO-2 →LUMO (14%) HOMO-2 →LUMO+1 (16%)
	272.34 (0.1273)	HOMO-1 →LUMO (18%)
	258.47 (0.2060)	HOMO-8 →LUMO (20%)
TPCz-C	381.41 (1.4601)	HOMO →LUMO (40%)
	322.32 (0.2864)	HOMO-1 →LUMO (29%) HOMO-1 →LUMO+1 (13%)
	295.49 (0.0237)	HOMO →LUMO+1 (26%)
	278.39 (0.1257)	HOMO-2 →LUMO (13%)
	271.02 (0.0705)	HOMO-3 →LUMO (11%)

		HOMO-1 →LUMO+1	(11%)
	258.83 (0.1572)	HOMO-3 →LUMO	(23%)
TPCz-D	425.16 (1.5270)	HOMO →LUMO	(44%)
	338.01 (0.2112)	HOMO-1 →LUMO	(36%
	286.13 (0.1261)	HOMO-2 →LUMO	(26%)
		HOMO →LUMO+1	(9%)
	272.85 (0.0335)	HOMO-5 →LUMO	(29%)
	268.74 (0.1443)	HOMO-3 →LUMO	(11%)
		HOMO-1 →LUMO+1	(13%)
	248.15 (0.0979)	HOMO-2 →LUMO+1	(10%)
		HOMO →LUMO+3	(13%)

Table S6. Optimised S_0 and S_1 geometries of **ICz-A** – **TPCz-D**, highlighting changes in bond lengths and bond angles.

Compound	Optimised geometry in S_0	Optimised geometry in S_1
ICz-A	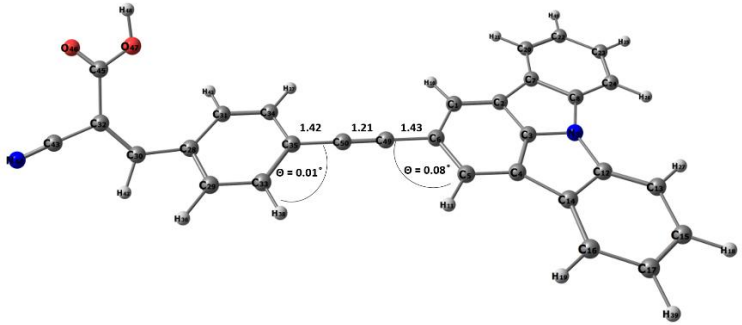	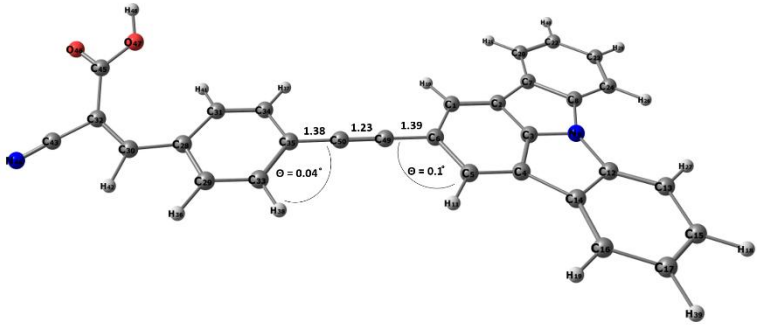
ICz-B	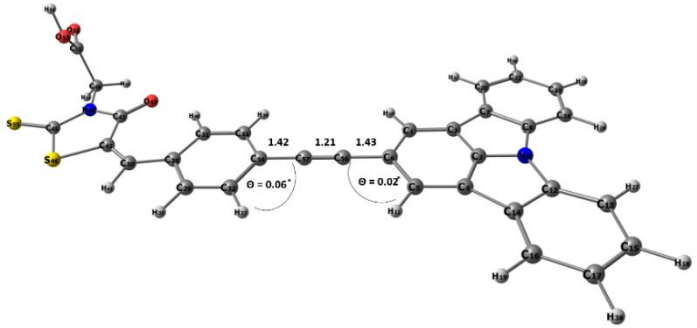	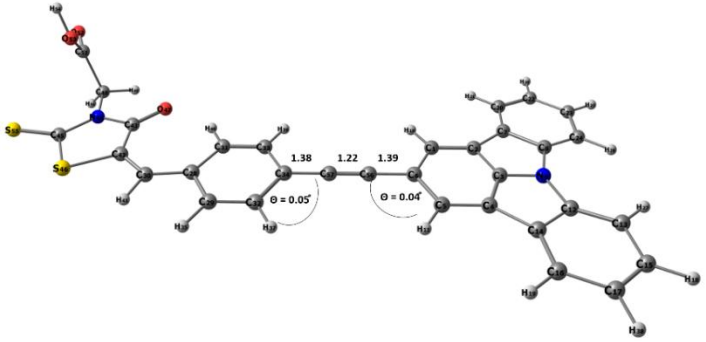
TPCz-A	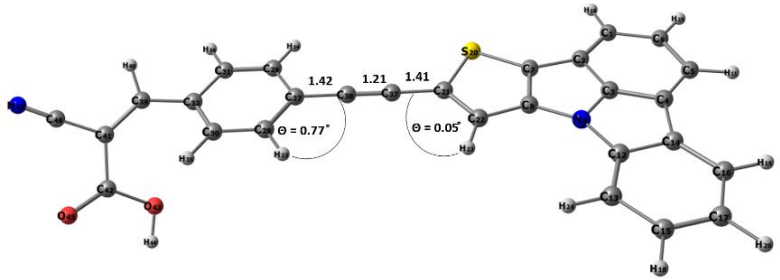	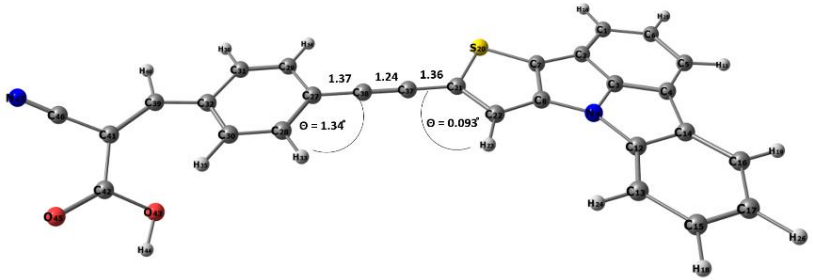

TPCz-B	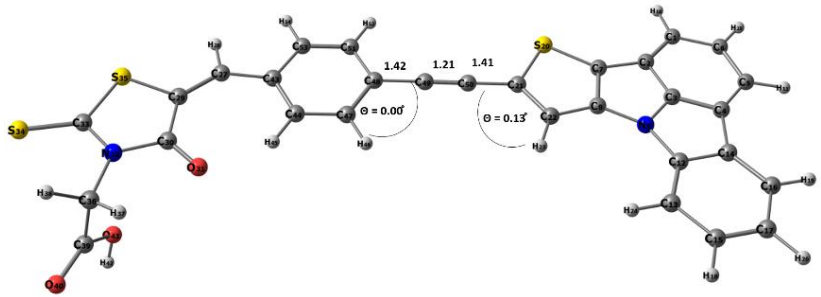	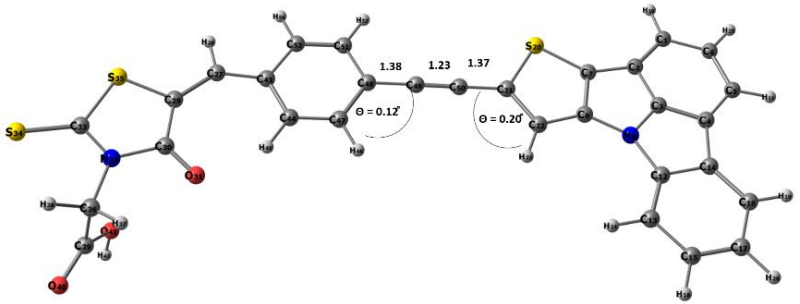
TPCz-C	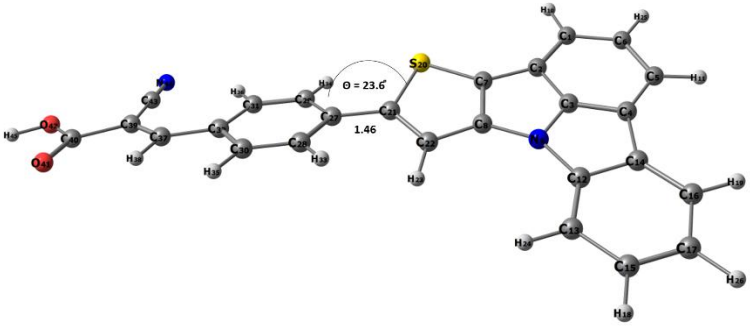	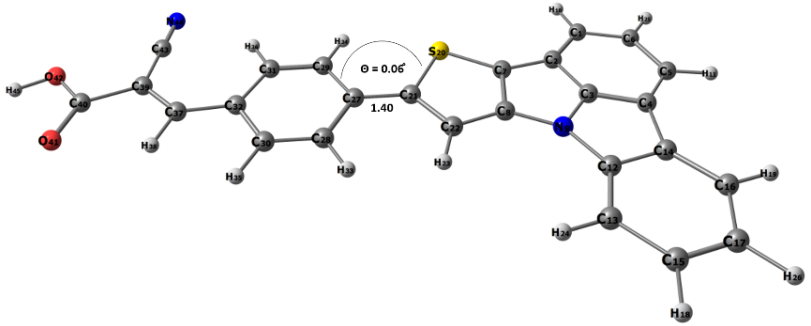
TPCz-D	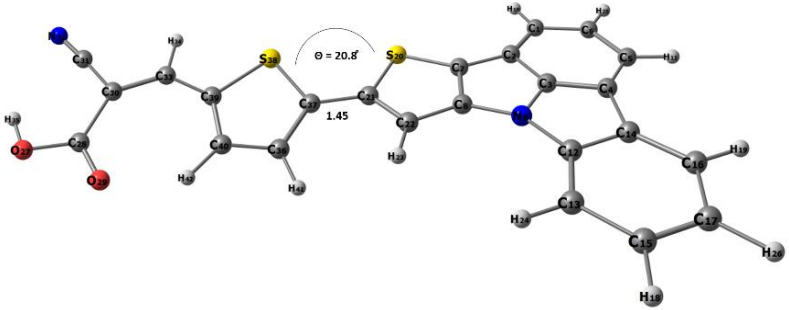	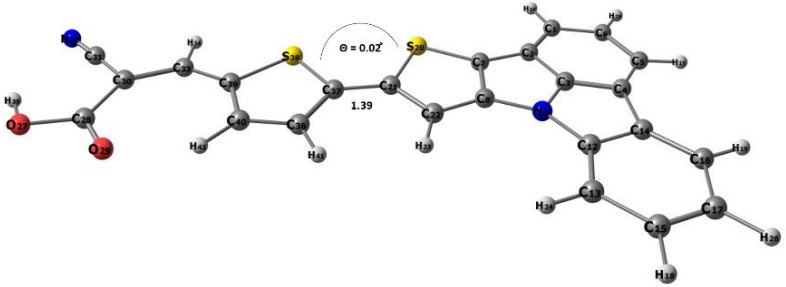

Table S7. TD-DFT calculated (6-311G(d,p)/B3LYP, DCM) absorption wavelength for **ICz-A** – **TPCz-D**.

Compound	Absorption [nm] (oscillator strengths)	Transitions
ICz-A	502.58 (1.0267)	HOMO →LUMO (49%)
	414.98 (0.2835)	HOMO-1 →LUMO (50%)
	350.76 (0.1377)	HOMO →LUMO+1 (45%)
	348.35 (0.4139)	HOMO-3 →LUMO (48%)
	302.97 (0.2827)	HOMO →LUMO+2 (43%)
	285.64 (0.0620)	HOMO-8 →LUMO (10%) HOMO-6 →LUMO (35%)
	279.51 (0.5588)	HOMO-2 →LUMO+1 (32%)
	270.21 (0.1601)	HOMO-2 →LUMO+1 (7%) HOMO →LUMO+5 (32%)
	264.56 (0.1682)	HOMO-3 →LUMO+1 (32%) HOMO →LUMO+4 (12%)
ICz-B	534.68 (1.2518)	HOMO →LUMO (50%)
	436.81 (0.3534)	HOMO-1 →LUMO (49%)
	391.08 (0.2000)	HOMO-3 →LUMO (48%)
	353.05 (0.1380)	HOMO →LUMO+2 (44%)
	338.78 (0.1010)	HOMO-5 →LUMO (17%) HOMO →LUMO+1 (30%)
	332.37 (0.2353)	HOMO-5 →LUMO (29%) HOMO →LUMO+1 (16%)
	288.87 (0.2412)	HOMO →LUMO+3 (36%)
	280.10 (0.1191)	HOMO-10 →LUMO (14%) HOMO →LUMO+4 (17%)
	277.34 (0.4080)	HOMO-2 →LUMO+2 (29%)
	269.32 (0.1913)	HOMO →LUMO+5 (37%)
	268.52 (0.1049)	HOMO →LUMO+6 (28%)
TPCz-A	526.66 (1.3941)	HOMO →LUMO (49%)
	459.99 (0.1628)	HOMO-1 →LUMO (49%)
	377.98 (0.2412)	HOMO →LUMO+1 (43%)
	349.60 (0.4273)	HOMO-3 →LUMO (13%) HOMO-1 →LUMO+1 (33%)
	338.18 (0.0816)	HOMO-3 →LUMO (30%) HOMO-1 →LUMO+1 (44%)
	314.17 (0.1142)	HOMO-2 →LUMO+1 (40%)
	305.77 (0.0748)	HOMO →LUMO+2 (39%)
	289.05 (0.0183)	HOMO-6 →LUMO (35%)
	259.78 (0.1428)	HOMO-2 →LUMO+2 (22%)
TPCz-B	556.23 (1.7113)	HOMO →LUMO (49%)
	469.80 (0.1382)	HOMO-1 →LUMO (49%)
	407.40 (0.4424)	HOMO-2 →LUMO (36%) HOMO →LUMO+1 (12%)
	353.67 (0.2728)	HOMO-1 →LUMO+1 (45%)
	322.64 (0.0768)	HOMO-4→LUMO (27%) HOMO-1 →LUMO+1 (16%)
	298.58 (0.1273)	HOMO-2→LUMO+1 (17%) HOMO →LUMO+3 (12%)
TPCz-C	508.65 (1.0596)	HOMO →LUMO (49%)
	460.59 (0.4089)	HOMO-1 →LUMO (49%)
	354.15 (0.0450)	HOMO →LUMO+1 (43%)
	331.26 (0.4676)	HOMO-3 →LUMO (21%0 HOMO-1 →LUMO+1 (26%)
	304.40 (0.0452)	HOMO-5 →LUMO (19%) HOMO-4 →LUMO (24%)
	295.57 (0.1503)	HOMO-2 →LUMO+1 (42%)
	253.65 (0.1164)	HOMO-8 →LUMO (10%) HOMO-1 →LUMO+3 (29%)
TPCz-D	538.94 (1.2451)	HOMO→LUMO (49%)
	486.06 (0.3913)	HOMO-1→LUMO (48%)
	343.38 (0.1102)	HOMO-3→LUMO (24%)

	364.38 (0.0676)	HOMO→LUMO+1 (12%) HOMO-3→LUMO (18%) HOMO→LUMO+1 (30%)
	322.62 (0.0737)	HOMO-5→LUMO (14%) HOMO-1→LUMO+1 (27%)
	252.79 (0.1502)	HOMO-2→LUMO+2 (17%)

Table S8. The optimised structures of dye–TiO_2 complexes calculated at the CAM-B3LYP/LANL2DZ/6-31G(d,p) level in DCM, with molecular orbital contours (isovalue = 0.03) for HOMO–1, HOMO, LUMO, and LUMO+1, their corresponding energies and energy gaps (E_{HOMO}-E_{LUMO}).

dye-(TiO_2)	HOMO-1 [eV]	HOMO [eV]	LUMO [eV]	LUMO+1 [eV]	ΔE [eV]
ICz-A@TiO_2	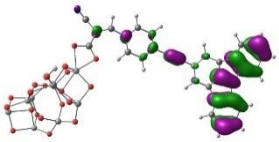	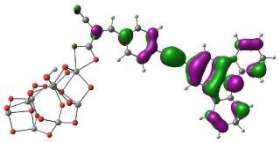	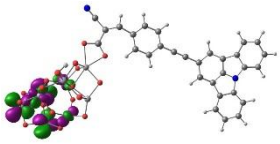	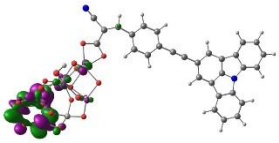	4.75
	-7.36	-6.73	-1.98	-1.83	
ICz-B@TiO_2	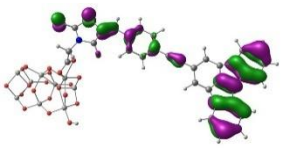	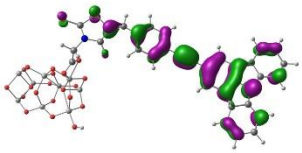	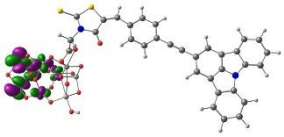	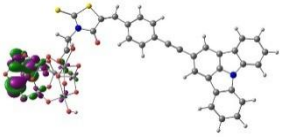	4.69
	-7.26	-6.65	-1.96	-1.8	
TPCz-A@TiO_2	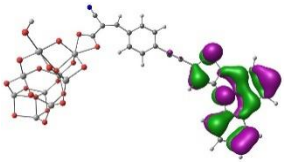	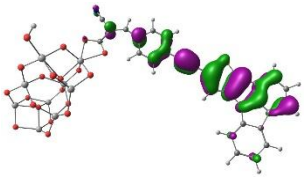	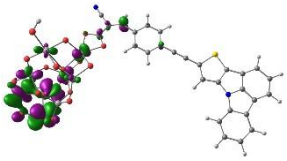	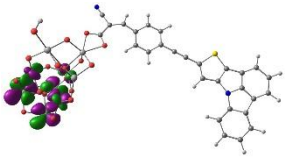	4.73
	-7.19	-6.73	-2.00	-1.85	
TPCz-B@TiO_2	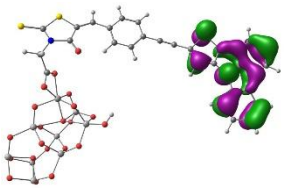	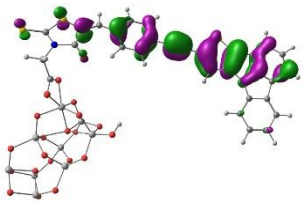	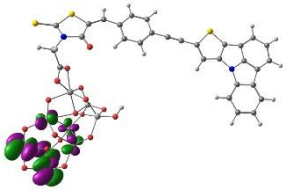	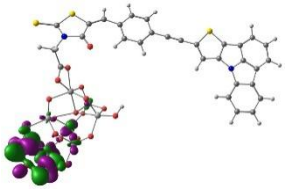	4.65
	-7.08	-6.64	-1.99	-1.83	
TPCz-C@TiO_2	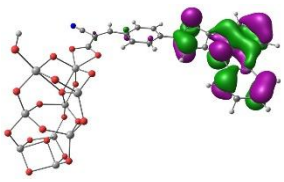	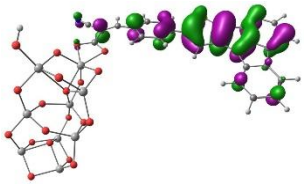	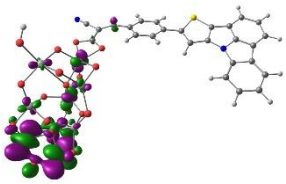	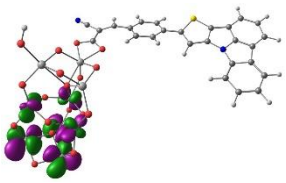	4.82
	-7.11	-6.81	-1.99	-1.83	

TPCz-D@TiO$_2$

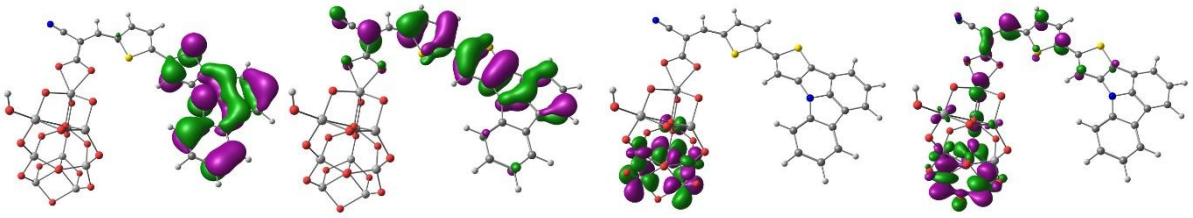

4.71

-7.15 -6.69 -1.98 -1.83

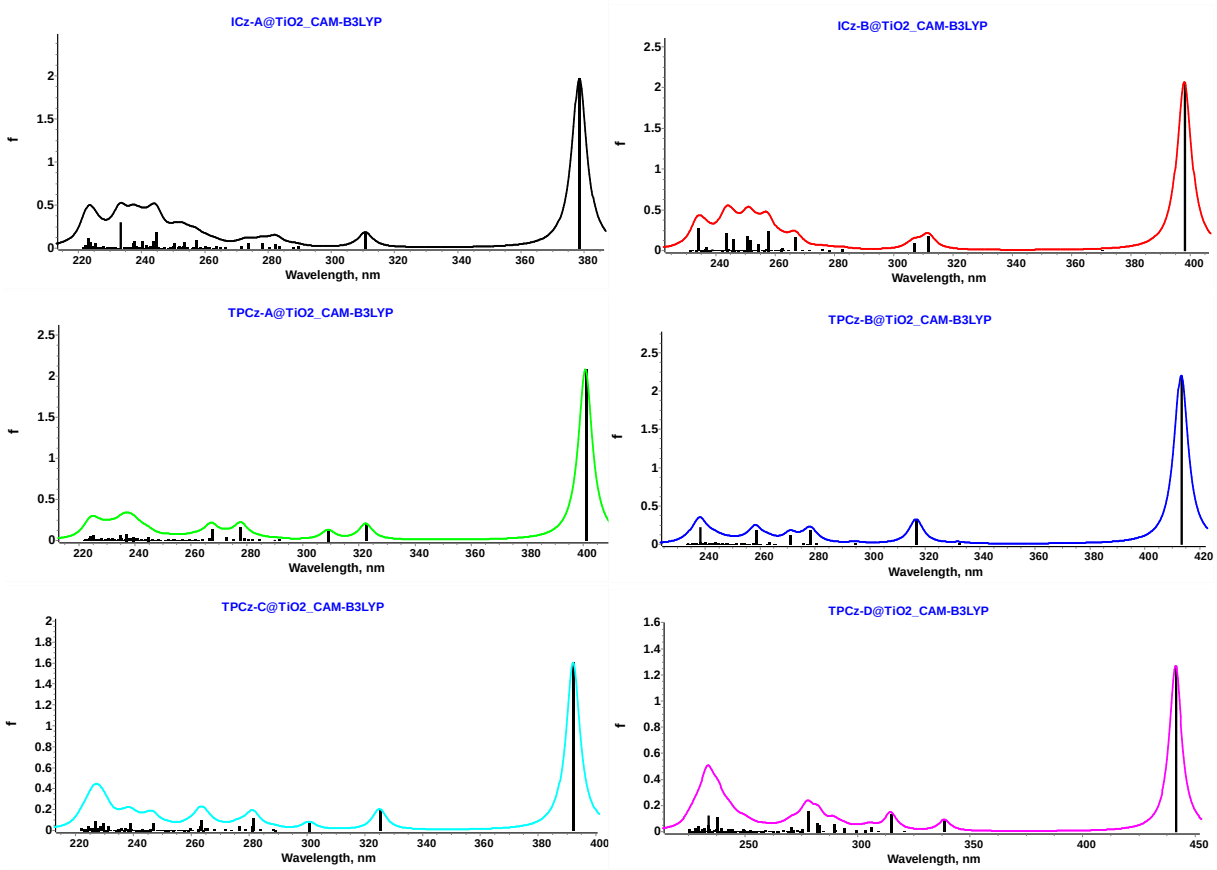

Fig. S3. TD-DFT (CAM-B3LYP/LANL2DZ;6-31G(d,p)) calculated absorption spectra of dyes **ICz-A** – **TPCz-D** dyes anchored to $(TiO2)_9$ cluster.

Electrochemical investigations

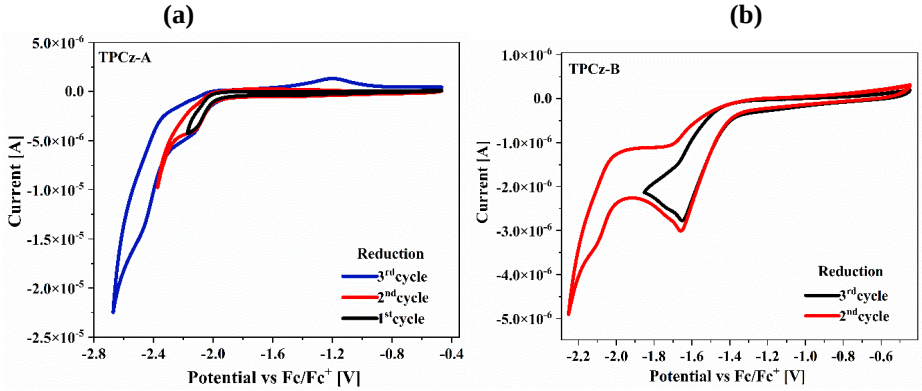

Fig. S4. Voltammograms of reduction processes of (a) **TPCz-A**, and (b) **TPCz-B** by cyclic voltammetry (CV) (Pt, CH_2Cl_2, $1 \cdot 10^{-1}$ mol·dm^{-3} Bu_4NPF_6, scan rate of 100 mV·s^{-1}).

Table S9. Next reduction and oxidation potentials (E_{red}, E_{ox} vs Fc/Fc^+).

Molecule	Method	E_{red}^2 [V]	E_{red}^3 [V]	E_{ox}^2 [V]	E_{ox}^3 [V]
ICz-A	CV	-2.11	-2.50	1.41	-
	DPV	-2.16	-2.44	1.32	-
ICz-B	CV	-	-	1.34	-
	DPV	-	-	1.29	-
TPCz-A	CV	-2.12	-2.48	1.48	-
	DPV	-2.08	-2.41	1.38	-
TPCz-B	CV	-2.09	-	1.06	1.44
	DPV	-2.07	-	1.01	1.34
TPCz-C	CV	-	-2.39	-	-
	DPV	-2.13	-2.31	-	-
TPCz-D	CV	-	-	1.42	-
	DPV	-	-	1.39	-

Solvent: CH_2Cl_2 with concentration $1 \cdot 10^{-3}$ mol·dm^{-3} and electrolyte Bu_4NPF_6 with concentration $1 \cdot 10^{-1}$ mol·dm^{-3}, Pt as the working electrode. Irreversible processes. E_{ox} – oxidation processes, E_{red} – reduction processes.

Photovoltaic parameters

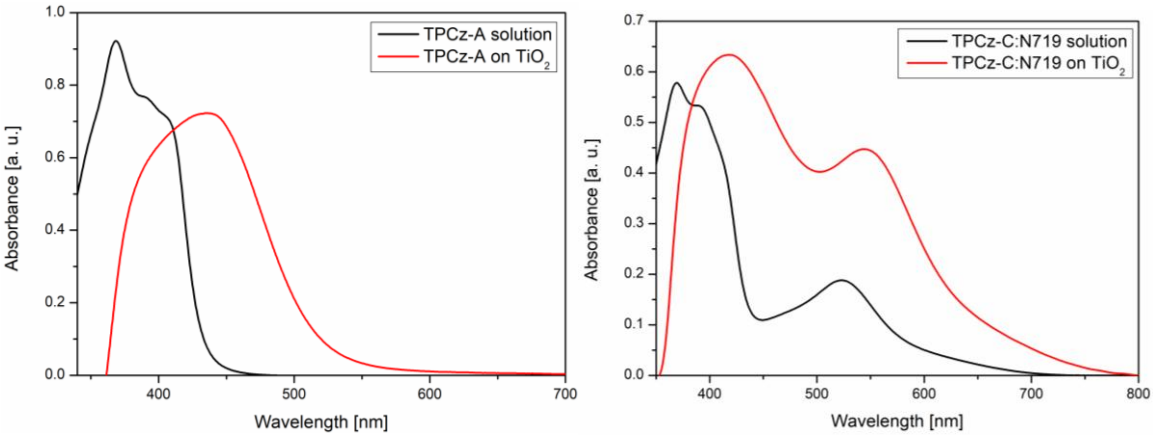

Fig. S5. The UV-Vis absorption of tested dyes in solution and anchored to TiO_2.

Table S10. Photovoltaic parameters of selected solar cells based on pyrrolo[3,2,1-jk]carbazole derivatives under reduced illumination conditions.

Photoanode structure	Light intensity [mW cm^{-2}]	V_{oc} [mV]	J_{sc} [mA cm^{-2}]	FF	PCE [%]
Glass/m-TiO_2@N719	100	749	14.96	0.53	5.88
	80	734	11.91	0.56	6.14
	60	723	8.99	0.62	6.72
	40	711	6.24	0.67	7.35
	20	692	3.37	0.73	8.50
	10	677	2.11	0.77	10.72

Glass/m-TiO_2@ICz-A	100	557	0.49	0.55	0.14
	80	538	0.37	0.53	0.13
	60	510	0.26	0.51	0.12
	40	472	0.17	0.50	0.10
	20	404	0.08	0.47	0.08
	10	356	0.05	0.46	0.08
Glass/m-TiO_2@TPCz-A	100	600	1.61	0.57	0.54
	80	601	1.35	0.58	0.59
	60	588	1.00	0.57	0.57
	40	569	0.67	0.56	0.54
	20	529	0.37	0.52	0.50
	10	487	0.21	0.51	0.52
Glass/m-TiO_2@TPCz-C	100	601	4.05	0.55	1.33
	80	613	3.52	0.58	1.61
	60	605	2.81	0.58	1.63
	40	599	1.87	0.58	1.64
	20	563	1.03	0.56	1.61
	10	534	0.62	0.56	1.77
Glass/m-TiO_2@TPCz-D	100	568	2.46	0.56	0.79
	80	568	2.17	0.58	0.92
	60	560	1.73	0.59	0.95
	40	544	1.19	0.59	0.95
	20	511	0.65	0.56	0.90
	10	484	0.38	0.57	1.02

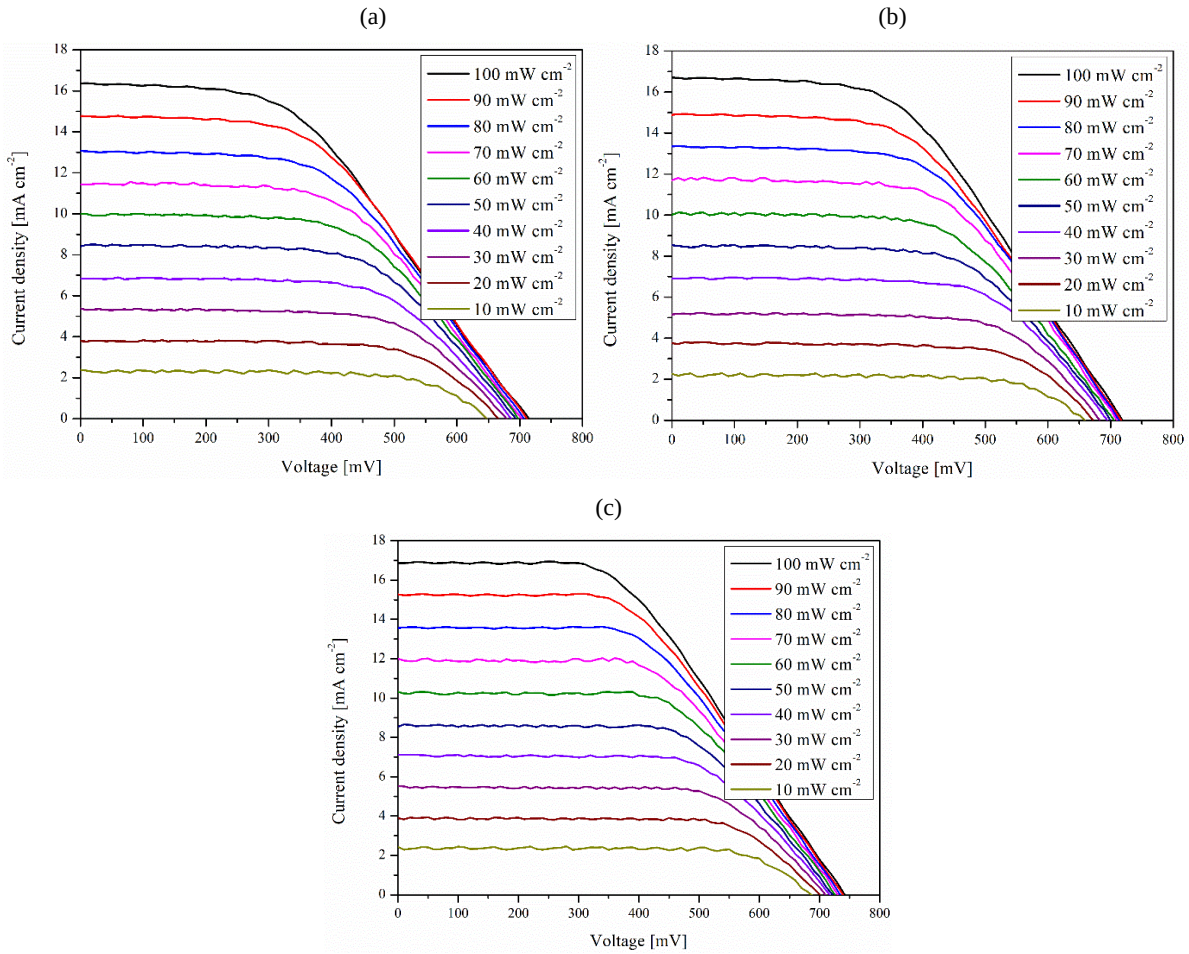

Fig. S6. Current density – voltage curves of DSSCs (a) glass/m-TiO_2@TPCz-C:N719, (b) glass/m-TiO_2@TPCz-C:N719:CDCA and (c) glass/BL/m-TiO_2@TPCz-C:N719:CDCA.

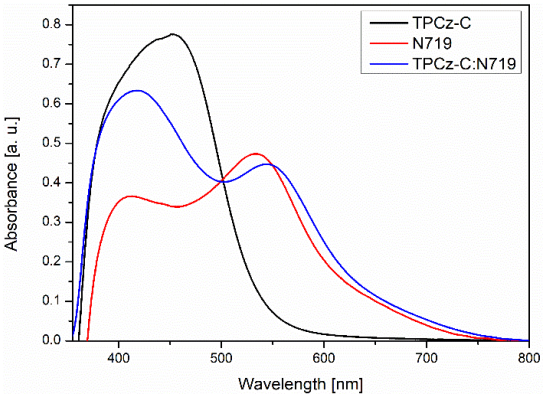

Fig. S7. UV-vis spectra of **TPCz-C**, N719 and its mixtures anchored to TiO_2

References

[1] P. Bujak, I. Kulszewicz-Bajer, M. Zagorska, V. Maurel, I. Wielgus, A. Proń, „Polymers for electronics and spintronics“, *Chem. Soc. Rev*., **2013**, *42*, 8895.

[2] Gaussian 16, Revision C.01, M. J. Frisch, G. W. Trucks, H. B. Schlegel, G. E. Scuseria, M. A. Robb, J. R. Cheeseman, G. Scalmani, V. Barone, G. A. Petersson, H. Nakatsuji, X. Li, M. Caricato, A. V. Marenich, J. Bloino, B. G. Janesko, R. Gomperts, B. Mennucci, H. P. Hratchian, J. V. Ortiz, A. F. Izmaylov, J. L. Sonnenberg, D. Williams-Young, F. Ding, F. Lipparini, F. Egidi, J. Goings, B. Peng, A. Petrone, T. Henderson, D. Ranasinghe, V. G. Zakrzewski, J. Gao, N. Rega, G. Zheng, W. Liang, M. Hada, M. Ehara, K. Toyota, R. Fukuda, J. Hasegawa, M. Ishida, T. Nakajima, Y. Honda, O. Kitao, H. Nakai, T. Vreven, K. Throssell, J. A. Montgomery, Jr., J. E. Peralta, F. Ogliaro, M. J. Bearpark, J. J. Heyd, E. N. Brothers, K. N. Kudin, V. N. Staroverov, T. A. Keith, R. Kobayashi, J. Normand, K. Raghavachari, A. P. Rendell, J. C. Burant, S. S. Iyengar, J. Tomasi, M. Cossi, J. M. Millam, M. Klene, C. Adamo, R. Cammi, J. W. Ochterski, R. L. Martin, K. Morokuma, O. Farkas, J. B. Foresman, and D. J. Fox, Gaussian, Inc., Wallingford CT, **2016**.

[3] G. Scalmani, M.J. Frisch, “Continuous surface charge polarisable continuum models of solvation. I. General formalism”, *J. Chem. Phys*., **2010**, *132*,114110.

[4] L.V. Skripnikov, Chemissian Visualization Computer Program, 2016, 4, 43, www.chemissian.com